Topological elementary equivalence of regular semi-algebraic sets in three-dimensional space

Floris Geerts[1] and **Bart Kuijpers**[2, *]

[1] University of Antwerp, Dept. of Mathematics and Computer Science, Middelheimlaan 1, Antwerpen, B-2020, Belgium.

[2] Hasselt University and transnational University Limburg, Databases and Theoretical Computer Science Research Group, Agoralaan, Gebouw D, Diepenbeek, B-3590, Belgium.

Received XXXX, revised XXXX, accepted XXXX
Published online XXXX

Key words Spatial logics, First-order logic over the reals, Topological elementary equivalence
MSC (2010) 03B70, 03C07, 14P10, 57M99, 68P15

We consider semi-algebraic sets and properties of these sets that are expressible by sentences in first-order logic over the reals. We are interested in first-order properties that are invariant under topological transformations of the ambient space. Two semi-algebraic sets are called *topologically elementarily equivalent* if they cannot be distinguished by such topological first-order sentences. So far, only semi-algebraic sets in one and two-dimensional space have been considered in this context. Our contribution is a natural characterisation of topological elementary equivalence of regular closed semi-algebraic sets in three-dimensional space, extending a known characterisation for the two-dimensional case. Our characterisation is based on the local topological behaviour of semi-algebraic sets and the key observation that topologically elementarily equivalent sets can be transformed into each other by means of geometric transformations, each of them mapping a set to a first-order indistinguishable one.

1 Introduction and summary

1.1 Introduction and context

In the broad area of *spatial logics*, formal languages for describing and querying geometric entities and configurations are designed and their expressiveness and complexity properties are studied [1]. These logics are interpreted over classes of structures featuring geometrical objects and relations, and may be first-order or higher-order languages, or fragments thereof. The structures over which these logics are interpreted range over topological spaces, affine spaces, metric spaces, among others. Relations present in these structures can be topological (e.g., connectivity), affine (e.g., parallelism of lines), or metric (e.g., equidistance of points). Although this area was pioneered long time ago by Whitehead [2] and Tarski [3], it has attracted renewed interest in the past decades because of its applications in artificial intelligence, database theory, physics and philosophy.

In the present paper, we focus on first-order spatial logics motivated by applications in spatial databases, where they are used as query languages. One particular model studied in spatial databases is the *constraint database model* [4]. In this model, spatial data are described by systems of polynomial inequalities over the reals and are known as semi-algebraic sets [5]. First-order logic over the reals, for which Tarksi proved a quantifier-elimination property [6], serves as a language to express queries and properties of the spatial data. The theory of constraint databases is closely related to embedded finite model theory [7] and o-minimal model theory in particular [8].

One particular class of properties, studied extensively in constraint databases, is topological in nature [4,9–15]. In this context, a property is called *topological* if it is preserved under some class of topological transformations. In mereotopology [1] and constraint databases [4], it is common to work with homeomorphisms of the ambient (Euclidean) space. The crucial question is which topological properties are expressible in first-order logic over

* Corresponding author E-mail: bart.kuijpers@uhasselt.be, Phone: +32 476 74 19 39

the reals, since the latter is the basic query language in the constraint database model. Answering this question thus yields an understanding of the expressive power of first-order logic as a query language.

One aspect in studying the expressive power is the question of topological elementary equivalence: which spatial figures can be distinguished by topological first-order properties? Most results in this context concern closed semi-algebraic sets in $\mathbf{R}^2$ [9, 10, 12]. Apart from a conjecture (Conjecture 3.1 in [16]) for topological elementary equivalence of sets in $\mathbf{R}^n$, not much is known for sets in dimensions higher than two. In this paper, we consider topological elementary equivalence for sets in $\mathbf{R}^3$, restricted to the regular open (or closed) semi-algebraic sets. Regularity is a common assumption, also in mereotopology. In a broader context, topological elementary equivalence stems from model theory. Our work is therefore related to topological model theory [17–19].

1.2 Summary of results

In this paper, we work with semi-algebraic sets in the Euclidean space $\mathbf{R}^3$ [5] and study a topological equivalence relation of such sets, referred to as *topological elementary equivalence* [12]. This equivalence relation is defined in terms of topological invariants that can be expressed in first-order logic over the reals, augmented with a ternary relation symbol S that is used to represent the semi-algebraic set under consideration [4]. More specifically, a first-order sentence expresses a topological invariant if it is invariant under *ambient orientation-preserving homeomorphisms* of $\mathbf{R}^3$. In other words, if a semi-algebraic set A satisfies such a sentence, then any semi-algebraic set B that is (ambiently) homeomorphic to A, by means of an orientation-preserving homeomorphism, also satisfies this sentence. We refer to such invariants as *first-order topological properties*, and say that two sets are topologically elementary equivalent if and only if they have the same first-order topological properties. For example, a sentence that expresses that a set has a non-empty interior is a first-order topological property; but a sentence that expresses that a set contains a straight-line segment is not.

Clearly, the standard topological equivalence relation, based on ambient homeomorphisms, is finer than the equivalence relation considered in this paper. Indeed, if A and B are ambiently homeomorphic by means of an orientation-preserving homeomorphism, then they are also topological elementary equivalent. The converse, however, is not true. Indeed, as our main result implies, there exists a connected set A and a disconnected set B in $\mathbf{R}^3$ that satisfy exactly the same set of first-order topological sentences. As a consequence, topological connectivity is not first-order expressible, neither by a single sentence nor by a countable family of sentences. For the two-dimensional case this was already known [20–22]. For example, it is known that the connectivity of sets is not a first-order topological property [20–22]. Similarly, the topological equivalence relation based on first-order properties that are invariant under general, not necessarily orientation-preserving, ambient homeomorphisms is finer than the topological elementary equivalence relation, but coarser than the standard topological equivalence relation.

In this paper, we characterise topological elementary equivalence for so-called *regular closed* semi-algebraic sets in $\mathbf{R}^3$, that is, sets that coincide with the closure of their interior. More specifically, we establish the following result.

> *Let A and B be two regular closed semi-algebraic sets in $\mathbf{R}^3$. Then, A and B are topologically elementary equivalent if and only if A can be transformed into B by means of a finite sequence of cylindrical replacements, $3d$-tube cut&paste transformations, complement $3d$-tube cut&paste transformations, wire cut&paste transformations, wire unknotting transformations, local surgeries, and orientation-preserving ambient homeomorphisms.*

All transformations mentioned here (apart from cylindrical replacement) are depicted in Figures 6, 7 and 9, and are described in full detail in Section 4.

Furthermore, we provide another characterisation of topological elementary equivalence that avoids transformations altogether and directly relates to first-order topological properties. More specifically, this characterisation is based on a well-known topological property of semi-algebraic sets, namely that locally around each point they are "conical" [5], on the one hand, and on a characterisation of topological elementary equivalence of closed semi-algebraic sets in $\mathbf{R}^2$ [12], on the other hand.

More precisely, if we denote by $\text{Cone}(A, \bar{p})$ the cone with base $A \cap S^2(\bar{p}, \varepsilon)$ and top $\bar{p}$, for small enough ε, then locally around $\bar{p}$ the set A is ambiently homeomorphic to $\text{Cone}(A, \bar{p})$. Here, $S^2(\bar{p}, \varepsilon)$ denotes the sphere

with centre $\bar{p}$ and radius ε. We observe that the base of such a cone can be seen as a semi-algebraic set in $\mathbf{R}^2$ (after a suitable stereographic projection). We then have the following characterisation.

> *Let A and B be two regular closed semi-algebraic sets in $\mathbf{R}^3$. Then, A and B are topologically elementary equivalent if and only if there is a bijection $f : A \to B$ such that for any point $\bar{p} \in A$ and $f(\bar{p}) \in B$, the bases of Cone$(A, \bar{p})$ and Cone$(B, f(\bar{p}))$ are topologically elementary equivalent, when viewed as sets in $\mathbf{R}^2$.*

That is, topological elementary equivalence of sets in $\mathbf{R}^3$ can be characterized in terms of topological elementary equivalence of sets in $\mathbf{R}^2$, by transitioning to the bases of cones. We observe that this characterisation in terms of cones confirms the conjecture on topological elementary equivalence of sets in $\mathbf{R}^n$, stated in [16], in the restricted setting of regular closed semi-algebraic sets in $\mathbf{R}^3$.

1.3 Organisation of the paper

This paper is organised as follows. Basic definitions of semi-algebraic sets, first-order logic over the reals and topological elementary equivalence are given in Section 2. Next, in Section 3, we describe the topology of semi-algebraic sets in $\mathbf{R}$, $\mathbf{R}^2$ and $\mathbf{R}^3$ and recall the characterisation of topological elementary equivalence of sets in $\mathbf{R}$ and $\mathbf{R}^2$. Furthermore, in Section 3.5, we formally state our characterisation in terms of cones and provide part of its proof. In Section 4, we present the transformations, also used to characterise topological elementary equivalence, and show that these transformations preserve topological elementary equivalence. In Section 5, we show that semi-algebraic sets can be brought into a canonical form. This property underlies the proofs of our main results. Finally, in Section 6, we conclude the paper with a short discussion.

2 Preliminaries

In this section, we give the basic definitions concerning semi-algebraic sets and topological first-order sentences. We give all definitions for general dimension n, but we mainly use them for $n = 1, 2$ and 3, in this paper.

We denote the set of real numbers by $\mathbf{R}$ and the n-dimensional real space by $\mathbf{R}^n$, for $n \geq 1$. Moreover, we equip $\mathbf{R}^n$ with the standard Euclidean topology. Throughout this paper, we also use the symbol $\mathbf{R}$ to abbreviate the standard first-order structure $\langle \mathbf{R}, 0, 1, +, \times, < \rangle$ of the real ordered domain.

2.1 Semi-algebraic sets

A *semi-algebraic set in* $\mathbf{R}^n$ is a subset of $\mathbf{R}^n$ that is definable by a first-order formula (without parameters) over the alphabet $(0, 1, +, \times, <)$, viewed as an n-ary relation over the reals. Since first-order logic over the reals allows quantifier elimination [6], we observe that semi-algebraic sets can be defined by quantifier-free first-order formulas. This means that a semi-algebraic set in $\mathbf{R}^n$ is a Boolean combination (union, intersection and complement) of sets that are described by inequalities of the form $p(x_1, ..., x_n) > 0$, where p is a polynomial in the real variables $x_1, \ldots, x_n$ with integer coefficients.

A semi-algebraic set is called *compact* if it is topologically closed and bounded. A semi-algebraic set A is called *regular closed* if it equals the closure of its interior, that is, if $A = \overline{(A^\circ)}$. A semi-algebraic set A is called *regular open* if it equals the interior of its closure, that is, if $A = (\overline{A})^\circ$. In this paper, when we use the term *regular*, we refer to regular closed. We always assume that semi-algebraic sets are *bounded*.[1] The *border* ∂A of A is defined as $\overline{A} \setminus A^\circ$.

2.2 First-order logic over the reals

To describe properties of a semi-algebraic set A in $\mathbf{R}^n$, we use first-order logic over the alphabet $\mathcal{L} = (0, 1, +, \times, <, S)$, being the expansion of the language of the reals with an n-ary relation symbol S. A semi-algebraic subset A in $\mathbf{R}^n$ can be naturally viewed as a first-order structure over $\mathcal{L}$, namely the expansion $\langle \mathbf{R}, A \rangle$ of the structure $\mathbf{R}$ with A. Hence, the truth of a sentence $\varphi(S)$ over $\mathcal{L}$ in $\langle \mathbf{R}, A \rangle$ can be denoted by $A \models \varphi(S)$.

[1] The restriction to "bounded" sets is not essential. We discuss this issue in more detail in Section 6.

We remark that, since semi-algebraic sets are first-order definable in $\mathbf{R}$, the question of $A \models \varphi(S)$, given $\varphi(S)$ and a (quantifier-free) description of the semi-algebraic set A, is effectively decidable, because the first-order theory of $\mathbf{R}$ is decidable [6].

2.3 Topological elementary equivalence

We call two subsets A and B in $\mathbf{R}^n$ *homeomorphic* if there is a homeomorphism h of the ambient space $\mathbf{R}^n$ such that $h(A) = B$. A sentence $\varphi(S)$ is called *invariant under homeomorphisms* (abbreviated as $\mathcal{H}_n$*-invariant*), if for any two homeomorphic *semi-algebraic* sets A and B in $\mathbf{R}^n$, $A \models \varphi(S)$ if and only if $B \models \varphi(S)$.

Finally, two semi-algebraic subsets A and B in $\mathbf{R}^n$ are called $\mathcal{H}_n$*-equivalent* if for each $\mathcal{H}_n$-invariant sentence $\varphi(S)$, we have $A \models \varphi(S)$ if and only if $B \models \varphi(S)$. We remark that homeomorphic semi-algebraic sets are $\mathcal{H}_n$-equivalent, but as we will see later, the converse does not hold.

It is known (see, for example, [23]) that any homeomorphism h of $\mathbf{R}^n$ is either isotopic to the identity mapping (in which case h is orientation-preserving) or isotopic to a reflection of $\mathbf{R}^n$ (in which case h is orientation-reversing). We refer to an orientation-preserving homeomorphism of $\mathbf{R}^n$ as an *isotopy* of $\mathbf{R}^n$. We call two subsets A and B in $\mathbf{R}^n$ *isotopic* if there is an isotopy h of $\mathbf{R}^n$ such that $h(A) = B$. Hence, when A and B are homeomorphic, either A is actually isotopic to B, or A is isotopic to a mirror image of B. A sentence $\varphi(S)$ is called *invariant under isotopies* (abbreviated as $\mathcal{I}_n$*-invariant*), if for any two isotopic *semi-algebraic* sets A and B, we have $A \models \varphi(S)$ if and only if $B \models \varphi(S)$. Finally, two subsets A and B in $\mathbf{R}^n$ are called $\mathcal{I}_n$*-equivalent* if for each $\mathcal{I}_n$-invariant sentence $\varphi(S)$, we have $A \models \varphi(S)$ if and only if $B \models \varphi(S)$. Of course, isotopic semi-algebraic sets are $\mathcal{I}_n$-equivalent, but, as mentioned above, the converse is not true. More colloquially, we call $\mathcal{I}_n$-equivalent sets, *topologically elementarily equivalent*.

We remark that $\mathcal{I}_n$-invariance implies $\mathcal{H}_n$-invariance. The following property provides the link between $\mathcal{H}_n$-equivalence and $\mathcal{I}_n$-equivalence. We denote by ρ_n the orientation-reversing reflection $\rho_n : (x_1, ..., x_{n-1}, x_n) \mapsto (x_1, ..., x_{n-1}, -x_n)$ of $\mathbf{R}^n$. The property below trivially follows from the observation that an homeomorphism of $\mathbf{R}^n$ is either an isotopy, or the composition of an isotopy and a reflection (such as ρ_n) of $\mathbf{R}^n$.

Property 1 *Let A and B be semi-algebraic sets in $\mathbf{R}^n$. Then, A and B are $\mathcal{H}_n$-equivalent if and only if A and B are $\mathcal{I}_n$-equivalent or A and $\rho_n(B)$ are $\mathcal{I}_n$-equivalent.*

As a consequence, it suffices to focus solely on $\mathcal{I}_n$-equivalence in the remainder of the paper.

3 The topology of semi-algebraic sets

In this section, we describe the topological structure of *compact* semi-algebraic sets in $\mathbf{R}^1$ and $\mathbf{R}^2$ and of *bounded regular* semi-algebraic sets in $\mathbf{R}^3$, in more detail. To this aim, we use Whitney stratifications of semi-algebraic sets and their local topological structure. For compact sets in $\mathbf{R}^1$ and $\mathbf{R}^2$, we also recall the characterisation of topological elementary equivalence [12]. We end this section by stating the main result of this paper, that is, a characterisation of topological elementary equivalence for bounded, regular semi-algebraic sets in $\mathbf{R}^3$.

3.1 The Whitney stratification of semi-algebraic sets

Semi-algebraic sets allow many different kinds of decompositions, each of which shows that they behave in a nice and controlled manner [5]. The topological structure of semi-algebraic sets is best explained using the so-called Whitney-stratifications of semi-algebraic sets [5, 24]. We refer to the literature for the exact definition of Whitney-stratifications [5, 24] and only highlight those properties of these decompositions that are relevant for this paper.

Let A be a semi-algebraic set in $\mathbf{R}^n$. A *Whitney-stratification $\mathcal{Z}$ of A* is a partition of A into locally closed smooth submanifolds $Z_0, \ldots, Z_k$ of $\mathbf{R}^n$, called *strata*, such that adjacent strata satisfy certain regularity conditions, also known as the Whitney conditions, and $\dim(Z_i) = i$, for $1 \leq i \leq k$. Intuitively, strata in a Whitney-stratification are such that within each connected component of a stratum, points have the same topological type, as explained next.

We first introduce some more definitions. Let C be a semi-algebraic set in $\mathbf{R}^n$. The *cone* with base C and top $\bar{p}$, denoted by $\text{Cone}(C, \bar{p})$, is the set of points $\{\bar{x} \in \mathbf{R}^n \mid \exists t \in [0,1]\, \exists \bar{y} \in C, \bar{x} = t\bar{p} + (1-t)\bar{y}\}$. We denote the closed ball in $\mathbf{R}^n$ with centre $\bar{p}$ and radius ε, for $\varepsilon > 0$, by $B^n(\bar{p}, \varepsilon)$ and its bordering sphere by $S^{n-1}(\bar{p}, \varepsilon)$.

Furthermore, we say that two smooth submanifolds M_1 and M_2 of $\mathbf{R}^n$ *intersect transversally*, which we denote by $M_1 \pitchfork M_2$, if for any point $\bar{q}$ in $M_1 \cap M_2$ it is the case that $\mathrm{T}_{\bar{q}}M_1 + \mathrm{T}_{\bar{q}}M_2 = \mathbf{R}^n$.[2] Here, $\mathrm{T}_{\bar{q}}M_i$ denotes the tangent space of M_i in $\bar{q}$, for $i = 1, 2$. If $M_1 \pitchfork M_2$, then we necessarily have that $\dim(M_1) + \dim(M_2) = n$.

Let $\bar{p}$ be a point in a semi-algebraic set A in $\mathbf{R}^n$ and let $\mathcal{Z} = \{Z_0, \ldots, Z_k\}$ be a Whitney-stratification of A. Moreover, let Z be the (unique) stratum containing $\bar{p}$. Let M be a smooth submanifold of $\mathbf{R}^n$ that intersects transversally each stratum of $\mathcal{Z}$; intersects Z in the single point $\bar{p}$; and satisfies $\dim(Z) + \dim(M) = n$. Then, the *normal slice* $N(\bar{p}, \mathcal{Z}, \varepsilon)$ through the stratum Z at $\bar{p}$ is the set $N(\bar{p}, \mathcal{Z}, \varepsilon) = M \cap A \cap B^n(\bar{p}, \varepsilon)$, where ε is such that $S^{n-1}(\bar{p}, \varepsilon)$ transversally intersects each stratum in $\mathcal{Z}$ and each stratum in $\mathcal{Z} \cap M$. The *link* $L(\bar{p}, \mathcal{Z}, \varepsilon)$ of the stratum Z at $\bar{p}$ is the set $L(\bar{p}, \mathcal{Z}, \varepsilon) = M \cap A \cap S^{n-1}(\bar{p}, \varepsilon)$. It can be shown that the topological types of $N(\bar{p}, \mathcal{Z}, \varepsilon)$ and $L(\bar{p}, \mathcal{Z}, \varepsilon)$ are independent of the submanifold M [24]. It is thus safe to omit the chosen submanifold M from the notations $N(\bar{p}, \mathcal{Z}, \varepsilon)$ and $L(\bar{p}, \mathcal{Z}, \varepsilon)$. Furthermore, we have the following property.

Property 2 ([24]) *Let A be a semi-algebraic set in $\mathbf{R}^n$, $\bar{p}$ be a point in A, and $\mathcal{Z} = \{Z_0, \ldots, Z_k\}$ be a Whitney-stratification of A. There exists an $\varepsilon > 0$ such that*

- *$N(\bar{p}, \mathcal{Z}, \varepsilon)$ is ambiently isotopic to Cone$(L(\bar{p}, \mathcal{Z}, \varepsilon), \bar{p})$; and*
- *$A \cap B^n(\bar{p}, \varepsilon)$ is ambiently isotopic to $[0, 1]^s \times N(\bar{p}, \mathcal{Z}, \varepsilon)$, where $s = \dim(Z)$ and Z is the stratum in $\mathcal{Z}$ to which $\bar{p}$ belongs.*

Of particular interest for this paper are links of strata at points that belong to a zero-dimensional stratum. In this case, Property 2 implies that $L(\bar{p}, \mathcal{Z}, \varepsilon) = A \cap S^{n-1}(\bar{p}, \varepsilon)$ and $A \cap B^n(\bar{p}, \varepsilon)$ is ambiently isotopic to Cone$(A \cap S^{n-1}(\bar{p}, \varepsilon), \bar{p})$. We note that one can always consider a stratification $\mathcal{Z}$ such that a given $\bar{p}$ belongs to a zero-dimensional stratum. In this way, one retrieves the well-known topological property of semi-algebraic sets in $\mathbf{R}^n$, that says that they are *conical*, locally around each point [5].

Definition 3.1 *The cone of A in $\bar{p}$* is $L(\bar{p}, \mathcal{Z}, \varepsilon)$, such that ε satisfies the conditions of Property 2 and $\bar{p}$ belongs to a zero-dimensional stratum Z in $\mathcal{Z}$. Furthermore, any such ε is called a *cone radius of A in $\bar{p}$*.

3.2 The topology of compact semi-algebraic sets in R and their topological elementary equivalence

Compact semi-algebraic sets in $\mathbf{R}$ have a very simple structure. Indeed, a compact semi-algebraic set A in $\mathbf{R}$ is well-known to be isotopic to a collection of closed intervals and isolated points. This can also be seen by considering a Whitney-stratification $\mathcal{Z}$ of A. Clearly, each stratum $Z \in \mathcal{Z}$ is either (a) (homeomorphic to) an interval (in case $\dim(Z) = 1$ and the link is necessarily empty); (b) a point inside an interval (in case $\dim(Z) = 0$ and the cone consists of a two points); (c) an endpoint of an interval (in case $\dim(Z) = 0$ and the cone consists of a single point); or (d) an isolated point (in case $\dim(Z) = 0$ and the cone is empty). In Figure 1 (top), we depict a semi-algebraic set in $\mathbf{R}$ and a stratification $\mathcal{Z}$ (grey shaded lines) of this set. Points $\bar{p}_1$, $\bar{p}_2$, $\bar{p}_3$, $\bar{p}_4$, and $\bar{p}_5$ correspond to Cases (a), (b), (c), (c) and (d), respectively. In the same figure, we also show the normal slices and links for these points relative to the given stratification. For Case (c) one can further distinguish between the Case (c') when the cone is one point to the left (e.g., point $\bar{p}_4$ in Figure 1), or the Case (c") when the cone is one point to right (e.g., point $\bar{p}_3$ in Figure 1), according to the order relation $<$ on $\mathbf{R}$. This distinction is important when dealing with isotopies.

We remark that all four cone types (corresponding to the zero-dimensional strata cases ((b), (c'), (c"), and (d)) can be characterised by a formula in first-order logic over $\mathcal{L}$. For example, the interior points x of S are defined by the formula $\exists \varepsilon > 0 \big(\forall \varepsilon' \big(\varepsilon' < \varepsilon \rightarrow \forall y((x - y)^2 = (\varepsilon')^2 \rightarrow S(y))\big)\big)$. Indeed, all instantiations of the free variable x of this formula make up the interior of the one-dimensional set S. It is clear that the types of cones that appear in a compact one-dimensional semi-algebraic set can be summed up exhaustively in increasing order (using the order relation $<$ on $\mathbf{R}$). So, we obtain the following characterisation of topological elementary equivalence for sets in $\mathbf{R}$.

Theorem 3.2 ([12]) *Let A and B two compact semi-algebraic sets in $\mathbf{R}$. Then A and B are isotopic if and only if A and B are $\mathcal{I}_1$-equivalent.* □

[2] Let U and V be two subspaces of a vector space X; then the *sum* $U + V$ is the set of all vectors $u + v$ where $u \in U$ and $v \in V$. The set $U + V$ is a subspace of X.

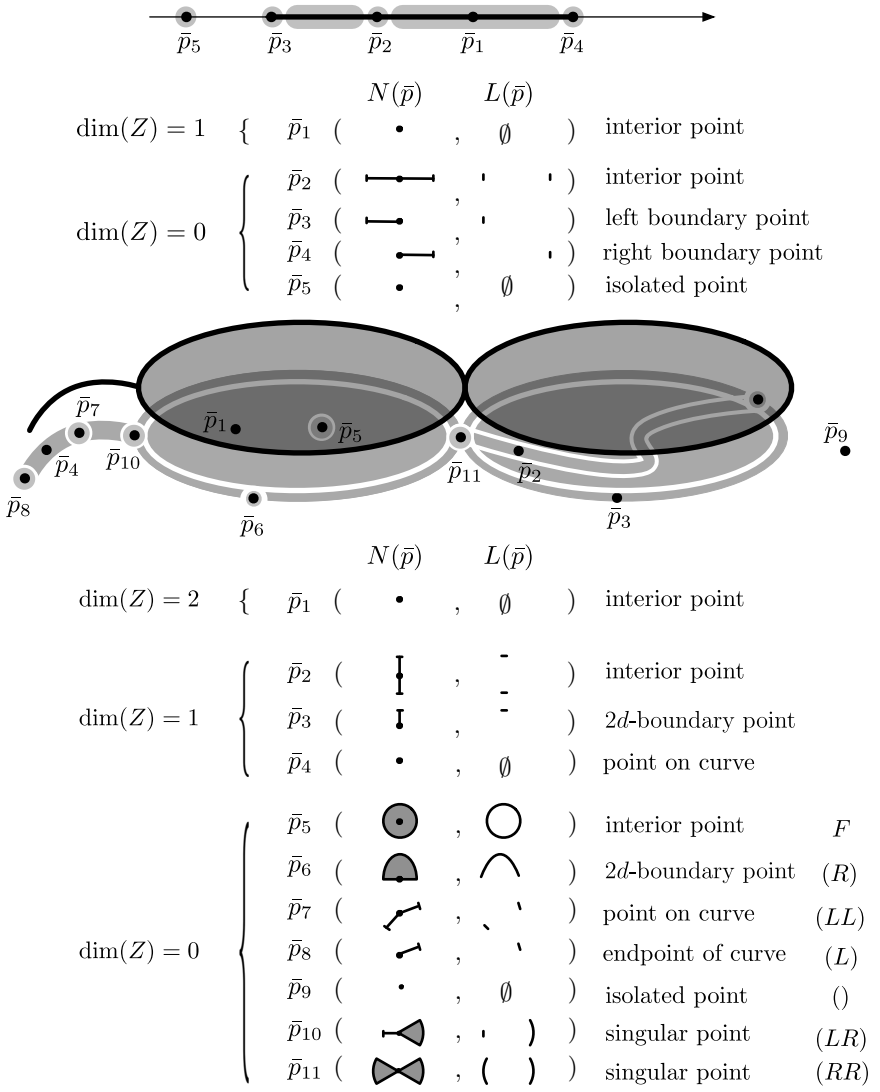

Fig. 1 Normal slices, links and cones of points in semi-algebraic sets in $\mathbf{R}$ (top) and $\mathbf{R}^2$ (bottom). Light shaded parts represent stratifications of the sets.

In combination with Property 1, we obtain that A and B are homeomorphic if and only if A and B are $\mathcal{H}_1$-equivalent.

3.3 The topology of compact semi-algebraic sets in $\mathbf{R}^2$ and their topological elementary equivalence

We next consider semi-algebraic sets in $\mathbf{R}^2$. Let A be a compact semi-algebraic set in $\mathbf{R}^2$ and let $\mathcal{Z}$ be a Whitney-stratification of A. Let $\bar{p}$ be a point of A and let $Z \in \mathcal{Z}$ be the stratum that contains $\bar{p}$. Then, depending on the dimension of Z and the link $L(\bar{p}, \mathcal{Z}, \varepsilon)$ of Z at $\bar{p}$, we distinguish between the following cases, also illustrated in Figure 1 (bottom). In that figure, we have lifted the semi-algebraic set in order to reveal the underlying stratification.

Interior points. If either $\dim(Z) = 2$ with empty link, $\dim(Z) = 1$ and the link consists of two points, or $\dim(Z) = 0$ and the cone is $S^1(\bar{p}, \varepsilon)$, then $\bar{p}$ is an interior point. These cases are illustrated in Figure 1 by points $\bar{p}_1$, $\bar{p}_2$, and $\bar{p}_5$, respectively.

$2d$-boundary points. If either $\dim(Z) = 1$ and the link consists of a single point, or $\dim(Z) = 0$ and the cone consists of a single closed arc segment on $S^1(\bar{p}, \varepsilon)$, then $\bar{p}$ is a point on a smooth border of the interior, also referred to as a *$2d$-boundary point*. These two cases are illustrated in Figure 1 by points $\bar{p}_3$ and $\bar{p}_6$, respectively.

Points on curves. Points on curves correspond to the case when either $\dim(Z) = 1$ and the link is empty, or $\dim(Z) = 0$ and the cone consists of two points. Points $\bar{p}_4$ and $\bar{p}_7$ in Figure 1 illustrate these two cases.

$2d$-singular points. Finally, the only remaining possible case is when $\dim(Z) = 0$ and the cone is either empty, or consists of a sequence of isolated points and closed arc segments, excluding the previous two cases. We call such points $2d$-singular points. In Figure 1, points $\bar{p}_8$, $\bar{p}_9$, $\bar{p}_{10}$, and $\bar{p}_{11}$ are $2d$-singular points.

Clearly, there are only a finite number of $2d$-singular points. We refer to the other types of points as *$2d$-regular points*. It is easy to see that if A contains a $2d$-regular point of a certain type, then it contains infinitely many of those points.

In [12], the following finite representation for cones of points in a semi-algebraic sets in $\mathbf{R}^2$ was introduced. The cones of interior points are represented by the letter F (for "full" circle). Any other cone is represented by a circular list of L's and R's (for "line" and "region", respectively), which describes the cone in a complete clockwise turn around the top. More specifically, each isolated point in the cone corresponds to an "L"; each closed arc segment corresponds to an "R". For example, the cones of $2d$-boundary points are represented by (R), the cones of points on curves by (LL), and the cones of points with empty cone are represented by the empty circular list $(\,)$. Similarly, the cones of the $2d$-singular points $\bar{p}_8$, $\bar{p}_9$, $\bar{p}_{10}$, and $\bar{p}_{11}$ in Figure 1 are represented by (L), $()$, (LR) and (RR), respectively.

We remark that in the case of a *regular* (closed) set A, cones can be either of type (F) or represented by a circular list containing k R's, for $k \geq 1$, abbreviated by (R^k). In other words, no L's appear in the cones of any point and neither do isolated points (with an empty cone) occur.

We represent the collection of all cones that occur in a semi-algebraic set A in $\mathbf{R}^2$ as a *multi-set* which consists of cones (represented as circular lists, as described above) together with their multiplicities. We represent multi-sets as follows. For example, for elements a and b and natural numbers n_1 and n_2, $\{\!\{a^{n_1}, b^{n_2}\}\!\}$ denotes the multi-set in which a and b occur n_1 and n_2 many times, respectively. We do allow these multiplicities to be infinite (∞). For example $\{\!\{a^{\infty}\}\!\}$ is the multi-set in which a occurs infinitely often.[3]

Definition 3.3 Let A be a compact semi-algebraic set in $\mathbf{R}^2$. The *point structure of* A, denoted by $\Pi_2(A)$, is the multi-set consisting of all (representations of) cones (circular lists) occurring in A.

For example, for the semi-algebraic set A shown in Figure 1, the point structure is given by $\Pi_2(A) = \{\!\{F^{\infty}, (R)^{\infty}, (LL)^{\infty}, (), (L), (LR), (RR)\}\!\}$.

The following characterisation for $\mathcal{I}_2$-equivalence (and for $\mathcal{H}_2$-equivalence via Property 1) of compact sets in $\mathbf{R}^2$ is established in [12].

Theorem 3.4 *Let A and B be two compact semi-algebraic sets in $\mathbf{R}^2$. Then A and B are $\mathcal{I}_2$-equivalent if and only if $\Pi_2(A) = \Pi_2(B)$.* □

Here, we use the standard notion of multi-set equality: two multi-sets are equal if and only if they both contain the same elements with the same multiplicities. Theorem 3.4 thus says that A and B are topologically elementarily equivalent if and only if each cone occurs exactly the same number of times in both A and B.

As a consequence, one disk in $\mathbf{R}^2$ is $\mathcal{I}_2$-equivalent to two disks in $\mathbf{R}^2$, illustrating that sets that are not isotopic can indeed be $\mathcal{I}_2$-equivalent.

[3] We use the symbol ∞ to mean "uncountably infinite", since semi-algebraic sets have cones that occur a finite or uncountably infinite number of times.

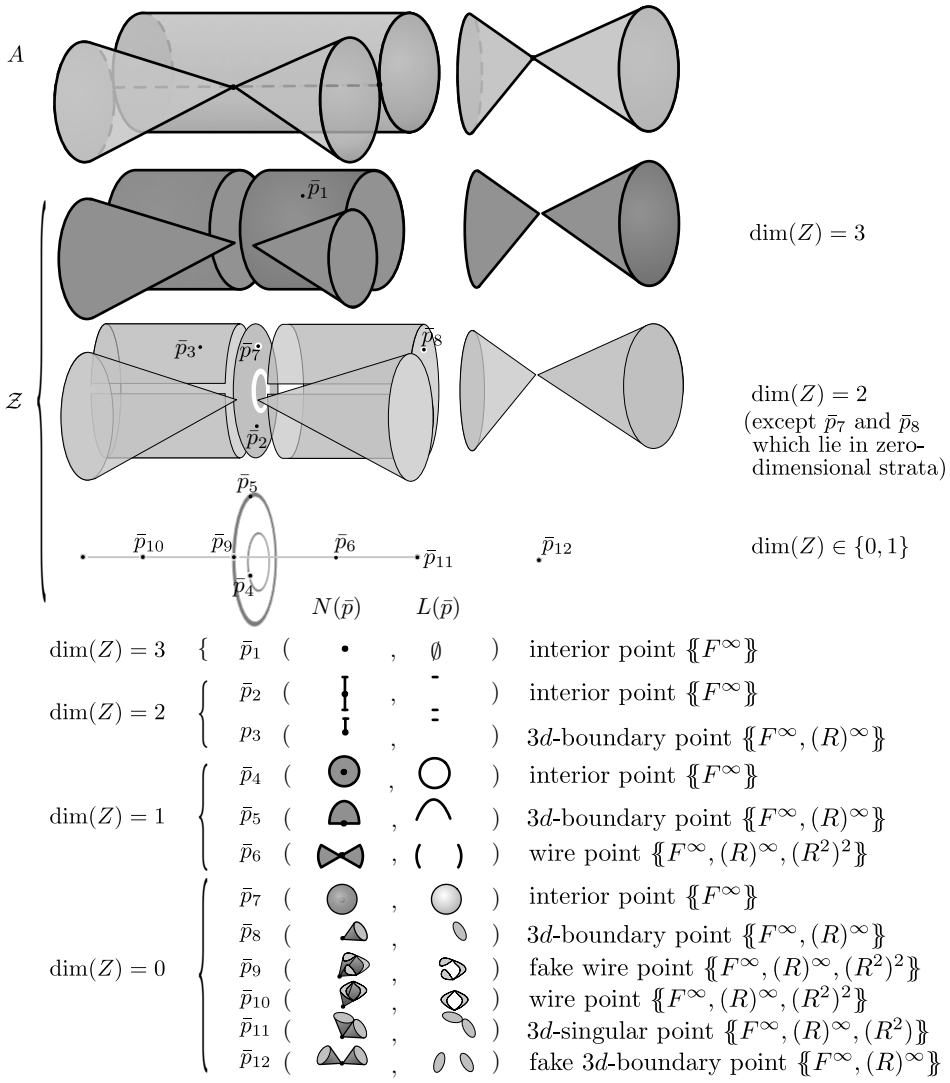

Fig. 2 A regular semi-algebraic set A in $\mathbf{R}^3$ and stratification $\mathcal{Z}$ of A. Points $\bar{p}_1$, $\bar{p}_2$, $\bar{p}_4$, and $\bar{p}_7$ are interior points, $\bar{p}_3$, $\bar{p}_5$ and $\bar{p}_8$ are $3d$-boundary points, $\bar{p}_6$ and $\bar{p}_{10}$ are wire points with profile $k = 2$, $\bar{p}_9$ is a fake wire point, $\bar{p}_{11}$ is a $3d$-singular point and $\bar{p}_{12}$ is a fake $3d$-boundary point.

3.4 The topology of regular semi-algebraic sets in $\mathbf{R}^3$

In this section, we describe the different kinds of cones that can appear in bounded regular (closed) semi-algebraic sets in $\mathbf{R}^3$. Let A be a bounded regular semi-algebraic set in $\mathbf{R}^3$ and let $\bar{p}$ be a point in A. We describe the different cone types based on the cone representation of semi-algebraic sets in $\mathbf{R}^2$, as described in the previous section. For this purpose, we regard the cone of a point $\bar{p}$, that is, $A \cap S^2(\bar{p}, \varepsilon)$, as a regular semi-algebraic set in $\mathbf{R}^2$ by projecting $S^2(\bar{p}, \varepsilon)$ stereographically onto a tangent plane through a point whose antipodal point is not in A. We denote this projection by σ_2 and hence $\sigma_2(A \cap S^2(\bar{p}, \varepsilon))$ is the two-dimensional result of projecting $A \cap S^2(\bar{p}, \varepsilon)$ using σ_2.

We remark that, with the exception of interior points, $\sigma_2(A \cap S^2(\bar{p}, \varepsilon))$ is a regular and compact semi-algebraic set in $\mathbf{R}^2$. For interior points, no antipodal point outside of A can be chosen (the cone consists of $S^2(\bar{p}, \varepsilon)$). In this case, we choose an arbitrary antipodal point and $\sigma_2(A \cap S^2(\bar{p}, \varepsilon))$ is the two-dimensional plane. We use the

following "finite" representation for the cone $A \cap S^2(\bar{p}, \varepsilon)$ of a point $\bar{p}$. We encode the cone $A \cap S^2(\bar{p}, \varepsilon)$ as the point structure $\Pi_2(\sigma_2(A \cap S^2(\bar{p}, \varepsilon)))$ of $\sigma_2(A \cap S^2(\bar{p}, \varepsilon))$.

Before defining the point structure of a semi-algebraic set A in $\mathbf{R}^3$, we describe the different kinds of points that can occur in A. Let $\bar{p}$ be a point of A and let $\mathcal{Z}$ be a Whitney-stratification of A. Let $Z \in \mathcal{Z}$ be the stratum containing $\bar{p}$. In Figure 2, we show a semi-algebraic set A in $\mathbf{R}^3$ and a Whitney-stratification $\mathcal{Z}$ of A. In that figure, we group the strata together based on their dimension, starting from the strata of dimension three (top); two (middle); one (bottom); and zero (also bottom). Exceptions are points $\bar{p}_7$ and $\bar{p}_8$ that reside in zero-dimensional strata, although we show them together with the two-dimensional strata of A (middle). All these strata should be combined to obtain a stratification of A.

Interior points. If $\dim(Z) = 3$ with empty link, $\dim(Z) = 2$ and the link consists of two points, $\dim(Z) = 1$ and the link consists of a disk on $S^2(\bar{p}, \varepsilon)$, or $\dim(Z) = 0$ and the cone consists of the sphere $S^2(\bar{p}, \varepsilon)$, then clearly $\bar{p}$ is a interior point of A. If there exists an interior point, there are infinitely many of them. We refer to these points simply as as *interior points* and we say that their cone is "full". The encoding of the cone of such a point is the point structure $\Pi_2(\sigma_2(S^2(\bar{p}, \varepsilon)))$, which is the multi-set $\{\!\{F^\infty\}\!\}$ in which the symbol F appears infinitely many times. In Figure 2, the points $\bar{p}_1$, $\bar{p}_2$, $\bar{p}_4$, and $\bar{p}_7$ illustrate the four different cases that lead to an interior point of the set A.

$3d$-boundary points. In case that either $\dim(Z) = 2$ and the link consists of a single point, $\dim(Z) = 1$ and the link consists of a single closed arc segment on $S^2(\bar{p}, \varepsilon)$, or $\dim(Z) = 0$ and the cone consists of a closed disk in $S^2(\bar{p}, \varepsilon)$. In other words, $\bar{p}$ is a point on the boundary of the interior of A, where locally around $\bar{p}$, the boundary is a 2-manifold. Again, if A contains one such point, it must contain infinitely many of them. We refer to these points as *$3d$-boundary points* of A and the encoding of their cones is given by the multi-set $\{\!\{F^\infty, (R)^\infty\}\!\}$, in which both F and (R) appear infinitely often as two-dimensional cone types. Indeed, this is the cone representation of a closed disk in $\mathbf{R}^2$. In Figure 2, the points $\bar{p}_3$, $\bar{p}_5$ and $\bar{p}_8$ illustrate the three different cases that result in a $3d$-boundary point of the set A.

$3d$-regular points. The interior points and $3d$-boundary points of A are called the *$3d$-regular points* of A.

$2d$-membrane points. In regular semi-algebraic sets in $\mathbf{R}^3$, there are no points residing on $2d$-membranes or boundaries thereof. This implies that we do not have to consider the cases when $\dim(Z) = 2$ and empty link, $\dim(Z) = 1$ and link containing isolated points, or $\dim(Z) = 0$ and the cone consists of circles or closed arc segments on $S^2(\bar{p}, \varepsilon)$.

Point on curves and endpoints of curves. Similarly, a regular set cannot contain embeddings of circles, closed arc segments or endpoints thereof. This rules out cases in which $\dim(Z) = 1$ and empty link, and $\dim(Z) = 0$ and cones containing isolated points.

Next, we investigate the remaining possible cases when either $\dim(Z) = 1$ or $\dim(Z) = 0$.

Wire points. Assume that $\dim(Z) = 1$. Locally around $\bar{p}$, the set $A \cap B^3(\bar{p}, \varepsilon)$ is homeomorphic to $\mathbf{R} \times \text{Cone}(L(\bar{p}, \mathcal{Z}, \varepsilon), \bar{p})$. In view of the regularity assumption on A, we are only left with the case that $L(\bar{p}, \mathcal{Z}, \varepsilon)$ is not empty and consists of multiple closed arc segments. The same type of points can be obtained when $\dim(Z) = 0$ and the cone has a very particular form. Indeed, $\sigma_2(A \cap S^2(\bar{p}, \varepsilon))$ consists of two $2d$-singular points, $\bar{q}_1$ and $\bar{q}_2$ of the same type $(R^k) = (R\ R \cdots R)$ of k R's with $k \geq 2$, and such that k distinct filled regions run between $\bar{q}_1$ and $\bar{q}_2$ in $\sigma_2(A \cap S^2(\bar{p}, \varepsilon))$. Here, k corresponds to the number of closed arc segments in the link of $\bar{p}$ when $\dim(Z) = 1$. We call such points *wire points (with profile k)* of A and if they appear in A, then there are infinitely many of them.

The finite encoding of the cone of a wire point is again given by the point structure $\Pi_2(\sigma_2(A \cap S^2(\bar{p}, \varepsilon)))$, that is, it is represented by the multi-set $\{\!\{F^\infty, (R)^\infty, (R^k)^2\}\!\}$, which reflects that the cone has two $2d$-singular points of type (R^k).

A wire with profile $k = 2$ is illustrated by points $\bar{p}_6$ and $\bar{p}_{10}$ in Figure 2. The encoding of the cone of $\bar{p}_{10}$ is the multi-set $\{\!\{F^\infty, (R)^\infty, (R^2)^2\}\!\}$, which reflects that in $\sigma_2(A \cap S^2(\bar{p}_{10}, \varepsilon))$, the cone of $\bar{p}_{10}$, the two-dimensional cone (RR) appears twice.

Since we have exhausted the possibilities for $\dim(Z) = 1$, it remains to consider the remaining cases for $\dim(Z) = 0$.

$3d$-singular points, fake $3d$-boundary points and fake wire points. If $\dim(Z) = 0$ and the cone $\sigma_2(A \cap S^2(\bar{p}, \varepsilon))$ is not covered by any of the previous cases, then we distinguish between three types of points depending on whether or not their *stereographic projected cones* are topologically elementary equivalent (as semi-algebraic sets in $\mathbf{R}^2$) to one of the previous cases:

- *Fake wire points.* These are points for which $\Pi_2(\sigma_2(A \cap S^2(\bar{p}, \varepsilon)))$ is equal to $\{\!\{F^\infty, (R)^\infty, (R^k)^2\}\!\}$ for some $k > 1$, that is, the encoding of cones of wire points of profile k. In Figure 2, $\bar{p}_9$ is such a point. As can be verified from the figure, $\sigma_2(A \cap S^2(\bar{p}_9, \varepsilon))$ is indeed topological elementary equivalent to the stereographic projection of a cone corresponding to a wire point of profile $k = 2$. Furthermore, it is not a wire point since only one filled region connects the two $2d$-singular points in $\sigma_2(A \cap S^2(\bar{p}_9, \varepsilon))$.

- *Fake $3d$-boundary points.* There are points for which $\Pi_2(\sigma_2(A \cap S^2(\bar{p}, \varepsilon)))$ is given by $\{\!\{F^\infty, (R)^\infty\}\!\}$, that is, the encoding of cones of $3d$-boundary points. In Figure 2, $\bar{p}_{12}$ is such a point. As can be verified from the figure, $\sigma_2(A \cap S^2(\bar{p}_{12}, \varepsilon))$ consists of two disks and hence it is indeed topological elementary equivalent to the stereographic projection of a cone consisting of a single disk, that is, to the cone of a $3d$-boundary point.

- *$3d$-singular point.* These are all remaining points, that is, points whose stereographic projected cones contain $2d$-singular points, but which are not fake wire points. In Figure 2, $\bar{p}_{11}$ is such a point. Indeed, $\Pi_2(\sigma_2(A \cap S^2(\bar{p}_{11}, \varepsilon)))$ is equal to $\{\!\{F^\infty, (R)^\infty, (RR)\}\!\}$. In fact, for regular sets, the encoding of cones of $3d$-singular points is always equal to the union of $\{\!\{F^\infty\}\!\}$, $\{\!\{(R)^\infty\}\!\}$, and distinct multi-sets of the form $\{\!\{(R^{k_i})^{\ell_i}\}\!\}$ with $k_i > 1$, $\ell_i \geq 1$, excluding the case $\{\!\{F^\infty, (R)^\infty, (R^k)^2\}\!\}$, corresponding to wire points.

Since $\dim(Z) = 0$, there are only a finite number of these kinds of points. We remark that singular points with an empty cone, that correspond to isolated points, do not occur in a regular semi-algebraic set.

3.5 The main result

We are now ready to state the main theorem of this paper. The remainder of this paper is devoted to proving this theorem. First, we define the three-dimensional equivalent of the point structure of a regular semi-algebraic set in $\mathbf{R}^3$ in analogy with Definition 3.3 for sets in $\mathbf{R}^2$.

Definition 3.5 Let A be a bounded, regular semi-algebraic set in $\mathbf{R}^3$. The *point structure of A* is the multi-set of multi-sets, denoted by $\Pi_3(A)$, consisting of the point structures $\Pi_2(\sigma_2(A \cap S^2(\bar{p}, \varepsilon)))$, where ε is the cone radius of A in $\bar{p}$, for all $\bar{p} \in A$.

For example, for the semi-algebraic set A shown in Figure 2, its point structure is given by

$$\Pi_3(A) = \{\!\{\{\!\{F^\infty\}\!\}^\infty, \{\!\{F^\infty, (R)^\infty\}\!\}^\infty, \{\!\{F^\infty, (R)^\infty, (R^2)^2\}\!\}^\infty, \{\!\{F^\infty, (R)^\infty, (R^2)\}\!\}^2\}\!\},$$

indicating that there are infinitely many $3d$-regular points, infinitely many wire points of profile $k = 2$, and two $3d$-singular points.

Our main result, which is a three-dimensional version of Theorem 3.4 from [12] for regular sets in $\mathbf{R}^3$, is the following:

Theorem 3.6 *Let A and B be (compact) regular semi-algebraic sets in $\mathbf{R}^3$. Then, A and B are $\mathcal{I}_3$-equivalent if and only if $\Pi_3(A) = \Pi_3(B)$.* □

Again, we obtain a characterisation of $\mathcal{H}_3$-equivalence via Property 1 as a corollary. We remark that we cannot expect more distinctive power from first-order logic. In particular, we cannot expect to be able to distinguish non-isotopic cones and indistinguishable cones.

P r o o f. To prove the if-direction of Theorem 3.6, we introduce a number of transformations that allow us to locally modify regular semi-algebraic sets in $\mathbf{R}^3$. These transformations preserve $\mathcal{I}_3$-equivalence and are used to transform a regular semi-algebraic set into *canonical form*, which is such that $\mathcal{I}_3$-equivalent sets can be transformed into one and the same canonical set. Moreover, during the transformation process the point structure of the set is not changed. The idea of transforming a semi-algebraic set into canonical form was also used in [12] for the case of closed sets in $\mathbf{R}^2$. We describe the transformations that preserve $\mathcal{I}_3$-equivalence and detail how sets can be brought into canonical form in Sections 4 and 5, respectively.

To prove the only-if-direction of Theorem 3.6, we show next that an $\mathcal{I}_3$-invariant $\mathcal{L}$-sentence $\varphi(S)$ can be defined, such that, when $\Pi_3(A) \neq \Pi_3(B)$ holds, we have $A \models \varphi(S)$ and $B \not\models \varphi(S)$. This indeed implies that if A and B are $\mathcal{I}_3$-equivalent, then $\Pi_3(A)$ must be equal to $\Pi_3(B)$, as desired.

Let us first analyse the point structure $\Pi_3(A)$ for a regular semi-algebraic set A in $\mathbf{R}^3$. As previously discussed, only a finite number of distinct encodings of cones of points in A can occur: $3d$-interior points whose cone encoding is given by $\{\!\{F^\infty\}\!\}$, $3d$-boundary points whose cone encoding is given by $\{\!\{F^\infty, (R)^\infty\}\!\}$, wire points whose cone encodings are given by $\{\!\{F^\infty, (R)^\infty, (R^k)^2\}\!\}$ for some profile $k \geq 2$, and $3d$-singular points whose cone encodings are given by $\{\!\{F^\infty, (R)^\infty, (R^{k_1})^{n_1}, \ldots, (R^{k_\ell})^{n_\ell}\}\!\}$ for some $k_1, \ldots, k_\ell, n_1, \ldots, n_\ell$ with all $k_i > 1$ and $n_i \geq 1$, excluding the case of wire points (that is, $\ell = 1$ and $n_\ell = 2$).

Furthermore, we observe that the existence of a $3d$-singular point implies the existence of wire points of profiles listed in the cone encoding of the $3d$-singular point. Similarly, a wire point implies the existence of $3d$-boundary points and $3d$-interior points, and for compact regular semi-algebraic sets, the existence of $3d$-interior points implies the existence of $3d$-boundary points, and vice versa. This implies that $\Pi_3(A)$ can be completely characterised, as follows:

- if A contains $3d$-singular points or wire points, then it suffices to list the cone encodings of $3d$-singular points in A, taking multiple occurrences into account, together with a set of cone encodings of wire points in A of different profiles, one for each such profile. Furthermore, cone encodings of wire points only need to be listed separately if they do not already occur in the cone encoding of any $3d$-singular point in A.

- If A does neither contain $3d$-singular points nor wire points, then either $\Pi_3(A)$ is empty (in the case that A is empty) or all encodings in $\Pi_3(A)$ correspond to $3d$-regular points. In the latter case, it suffices to only consider a single point in A (if A is non-empty) with cone encoding $\{\!\{F^\infty\}\!\}$.

Hence, if we assume that $\Pi_3(A) \neq \Pi_3(B)$, then either A contains a $3d$-regular point whereas B does not, or vice versa; or A contains a wire point of profile k, whereas B does not, or vice versa; or there is particular cone type of a $3d$-singular point that occurs a different number of times in A than in B. It thus suffices to construct a first-order sentence that expresses that a semi-algebraic set in $\mathbf{R}^3$ has a certain number of points with cones of a pre-described type. Since the cone type is invariant under isotopies, such a sentence will be necessarily $\mathcal{I}_3$-invariant. Furthermore, it should be clear that it suffices to show that there is such a first-order formula $\psi_\tau(x, y, z, S)$ that expresses that point (x, y, z) has cone type τ in S. Such a formula ψ_τ can be constructed as follows:

- Let $\varphi_{cradius}(x, y, z, r, S)$ be a first-order formula that expresses that r is a cone radius for (x, y, z) in S. It is known that this can be expressed in first-order logic [25].

- Let $\varphi_{stereo}(x', y', x, y, z, r, S)$ be a first-order formula that returns the stereographic projection (in variables x' and y') of S intersected with a sphere with centre (x, y, z) and radius r. As previously explained, this projection is onto a tangent plane through a point whose antipodal point is not in A, if such a point exists, and an arbitrary antipodal point otherwise.

- In [12], it was shown that for any closed semi-algebraic set D in $\mathbf{R}^2$, with point structure the multi-set $\tau = \Pi_2(D)$, there exists a "characteristic" formula $\psi^2_\tau(S')$ that expresses that the binary predicate S', that represents a two-dimensional semi-algebraic set, has the same point structure as D. Basically, the formula ψ^2_τ enumerates the cone types that occur in D with their multiplicities. This implies that there exists a first-order formula $\varphi_\tau(x, y, z, r, S)$, such that for any semi-algebraic set A in $\mathbf{R}^3$, any point $\bar{p} \in \mathbf{R}^3$ and any real number $\varepsilon > 0$, we have $A \models \varphi_\tau(x, y, z, r, S)[\bar{p}, \varepsilon]$ if and only if the stereographic projection of the set $A \cap S^2(\bar{p}, \varepsilon)$ has point structure τ.

We can conclude that the formula $\psi_\tau(x, y, z, S)$, that we are looking for, is

$$\exists r\, \varphi_{cradius}(x, y, z, r, S) \wedge \varphi_\tau(x, y, z, r, S).$$

This concludes the proof. □

We observe the following. The characterisation of topological elementary equivalence given in Theorem 3.6 can be phrased as the characterisation given in the Introduction. Indeed, if $\Pi_3(A) = \Pi_3(B)$ then it is easily verified that there exists a bijection f from A to B such that $\Pi_2(\sigma_2(A \cap S^2(\bar{p}, \varepsilon))) = \Pi_2(\sigma_2(B \cap S^2(f(\bar{p}), \varepsilon)))$, for any point $\bar{p}$ in A and $\varepsilon > 0$ that is a cone radius for A and B in $\bar{p}$ and $f(\bar{p})$, respectively. By Theorem 3.4 this implies that $\sigma_2(A \cap S^2(\bar{p}, \varepsilon))$ is $\mathcal{I}_2$-equivalent to $\sigma_2(B \cap S^2(f(\bar{p}), \varepsilon))$, or in other words, that the bases of the cones $\text{Cone}(A, \bar{p})$ and $\text{Cone}(B, f(\bar{p}))$ are $\mathcal{I}_2$-equivalent when these are regarded as sets in $\mathbf{R}^2$. The latter trivially implies again that $\Pi_3(A) = \Pi_3(B)$, as desired.

Furthermore, the proof strategy of the if-direction of Theorem 3.6 reveals that $\Pi_3(A) = \Pi_3(B)$ if and only if A can be transformed into B by means of a sequence of transformations and isotopies. Indeed, A is to be transformed into a regular semi-algebraic set in canonical form with the same point structure as A. Similarly, for B. Since these transformations are reversible, when $\Pi_3(A) = \Pi_3(B)$, then A can indeed be transformed into B, via the canonical form. Since the transformations preserve the point structure, if A can be transformed into B, then $\Pi_3(A) = \Pi_3(B)$ must hold. Hence, as a corollary of Theorem 3.6, A is $\mathcal{I}_3$-equivalent to B if and only if A can be transformed into B, as desired.

We end this section with another corollary of Theorem 3.6, that says that $\mathcal{I}_3$- and $\mathcal{H}_3$-equivalence coincide for *regular* semi-algebraic sets in $\mathbf{R}^3$.

As we have already remarked in Section 2, it is well known that a homeomorphism of $\mathbf{R}^n$ ($n \geq 1$) is either (a) orientation preserving (and thus an isotopy) or (b) orientation reversing (and thus the composition of an isotopy and an orientation-reversing reflection, such as $\rho_n : (x_1, ..., x_{n-1}, x_n) \mapsto (x_1, ..., x_{n-1}, -x_n)$) [23]. From the description in Section 3.3 of the possible cone types of closed semi-algebraic sets in $\mathbf{R}^2$, we know that only the full cone and cones of type (R^k), for $k \geq 1$, can appear in a regular semi-algebraic sets in $\mathbf{R}^2$. In this setting, it is clear that these cones (and their encodings) are invariant under reflections of $\mathbf{R}^2$, such as ρ_2. This implies that, for a *regular* semi-algebraic set A in $\mathbf{R}^2$, also the point structure $\Pi_2(A)$ is invariant under orientation-reversing reflections. So, in particular, we have $\Pi_2(A) = \Pi_2(\rho_2(A))$. From Theorem 3.4, we can then see that $\mathcal{I}_2$- and $\mathcal{H}_2$-equivalence coincide for *regular* semi-algebraic set in $\mathbf{R}^2$. This is not true for arbitrary closed semi-algebraic sets in $\mathbf{R}^2$ [12].

We can lift this result for $\mathbf{R}^2$ to $\mathbf{R}^3$. Indeed, from the discussion in Section 3.4 of the possible cone types in a regular semi-algebraic set in $\mathbf{R}^3$, we recall that the cones of points in such sets can be seen as regular two-dimensional semi-algebraic sets (after a stereographical projection). Therefore, the orientation-reversing reflection ρ_3 of $\mathbf{R}^3$ maps cones of points in regular semi-algebraic sets to cones that have the same point structure (seen as a two-dimensional set). So, we can conclude that ρ_3 preserves the point structure of any regular semi-algebraic set A in $\mathbf{R}^3$, that is, $\Pi_3(A) = \Pi_3(\rho_3(A))$. Thus, if we have $\Pi_3(A) = \Pi_3(B)$, for two regular semi-algebraic sets A and B in $\mathbf{R}^3$, then we also obtain $\Pi_3(\rho_3(A)) = \Pi_3(A) = \Pi_3(B) = \Pi_3(\rho_3(B))$. This proves the following corollary.

Corollary 3.7 *Let A and B be (compact) regular semi-algebraic sets in $\mathbf{R}^3$. Then, A and B are $\mathcal{I}_3$-equivalent if and only if A and B are $\mathcal{H}_3$-equivalent.* □

4 $\mathcal{I}_3$-preserving transformations of regular semi-algebraic sets

The transformations that we describe in this section preform local transformations on regular semi-algebraic sets in $\mathbf{R}^3$. We always assume that these take place in some cube I^3, which we can take to be $[-2, 2]^3$, for instance, and we refer to I^3 as the *working cube* and to the square $[-2, 2]^2 \times \{0\}$ as the *working square* in $\mathbf{R}^3$, which we denote by $I^3_{z=0}$. Similarly, I^2 denotes the working square $[-2, 2]^2$ in $\mathbf{R}^2$. We remark that these cubes and squares are sometimes depicted in the figures in this section as beams and rectangles, respectively.

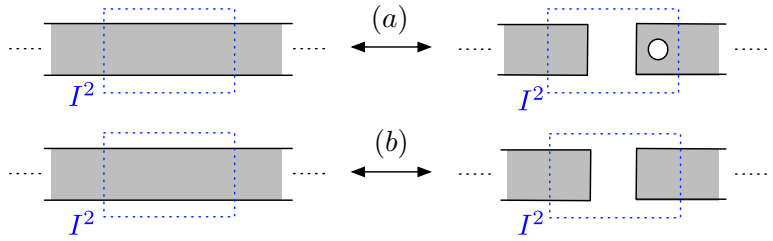

Fig. 3 The weak strip cut&paste (a) and the strip cut&paste (b) in $\mathbf{R}^2$. The dashed blue rectangular area depicts the working square I^2.

4.1 A review of transformations in $\mathbf{R}^2$

We start by providing some insights in the transformations of regular closed sets in $\mathbf{R}^2$, taken from [12], that are relevant for the proofs in this paper.

We first recall the *(weak) strip cut&paste* transformations which preserve $\mathcal{I}_2$-equivalence of regular sets in $\mathbf{R}^2$. These transformations are illustrated in Figure 3. The *strip cut* transformation (see Figure 3, (b) left to right), transforms regular sets locally within the working square I^2, depicted by the blue dashed lines. The transformation is applicable when the regular semi-algebraic set in $\mathbf{R}^2$ looks like a strip inside I^2, and the result of the transformation is that, within I^2, the strip is cut into two pieces. The *strip paste* transformation is the reverse transformation of the strip cut (see Figure 3, (b) right to left). In the *weak versions* of the strip cut&paste transformations, a hole is present in one of the resulting strips after the cut (see Figure 3, (a)). The weak strip cut&paste is of particular interest for our proofs and we give some more details about the proof showing that they preserve $\mathcal{I}_2$-equivalence (which can be found, in detail, in [12]).

The preservation of $\mathcal{I}_2$-equivalence is based on the inexpressibility of the decision problem MAJORITY about two finite sets R_1 and R_2 that is defined as MAJORITY(R_1, R_2) is true if and only if $R_1 \subseteq R_2$ and $|R_1| \leq 2|R_2|$. The decision problem MAJORITY(R_1, R_2) is not uniformly first-order expressible over the alphabet $(<, R_1, R_2)$ on finite ordered structures [20].[4] The reduction argument uses a geometric construction, for two given finite sets R_1 and R_2, as illustrated in Figure 4. Within a rectangular area J^2 in the working square I^2, R_1 is placed in the direction of the y-axis and R_2 is placed in the direction of the x-axis and on the $R_2 \times R_1$ raster, strips are constructed (in first-order logic), as shown in Figure 4. Outside J^2, but inside I^2, some fixed strips are added. We call the result $D(R_1, R_2)$ and its construction is such that this set is homeomorphic to the right hand side of Figure 3 (a) in case of majority and to the left hand side in the other case (see [12] for details).

The first-order inexpressibility of MAJORITY(R_1, R_2) implies that the weak strip cut&paste preserves $\mathcal{I}_2$-equivalence. To obtain that the strip cut&paste transformation of Figure 3 (b) preserves $\mathcal{I}_2$-equivalence another inexpressibility result on finite sets is used [12]. This reduction argument shows that inside the working square an isolated regular part of a set in $\mathbf{R}^2$ can be replaced by any other isolated regular part. Figure 5 shows the transformation process from the weak strip cut&paste to strip cut&paste: (a) a weak strip cut; (b) one disk is replaced by two disks; and (c) & (d) three more weak strip cut&paste operations.

4.2 Flower normal form

The strip cut&paste transformations allow the transformation of any compact and regular set in $\mathbf{R}^2$ into a canonical form, referred to as the *flower normal form*, which, in the presence of singular points consists of "flowers" with a number of "petals". The cone of the point $\bar{p}_{11}$ in Figure 1 is an example of a flower with $k = 2$ petals. In general, if the singular point has cone type (R^k), then it corresponds to a flower with k petals. If there are no singular points in a set, then the canonical form is either a disk or the empty set. The flower normal form thus represents all topological information in a set that can be identified by first-order logic, that is, each regular set A in $\mathbf{R}^2$ is $\mathcal{I}_2$-equivalent to a finite number of flowers, one for each singular point, or a single disk or empty

[4] Here and in some proofs, we also use formulas in the language of the reals expanded with additional relation symbols, as well as formulas in restrictions of the previous languages where $0, 1, +$, and $\times$ are not used. In all these cases, similar definitions and notations are used as in Section 2.

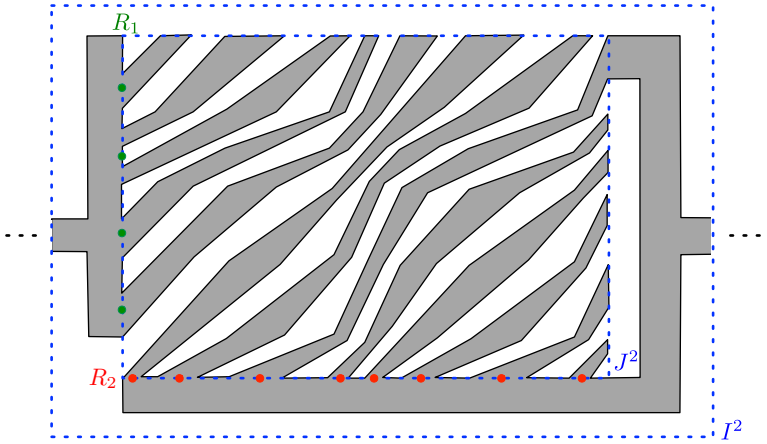

Fig. 4 The first-order construction of $D(R_1, R_2)$ in $\mathbf{R}^2$, given two finite sets R_1 and R_2.

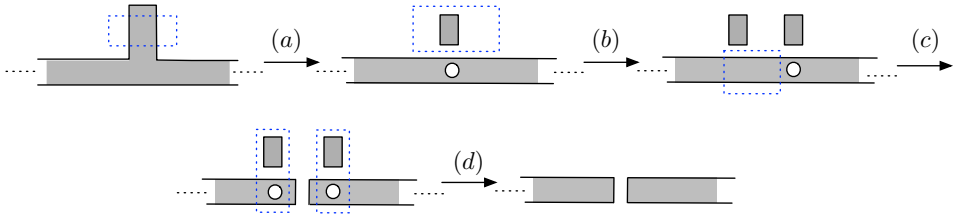

Fig. 5 The process from weak strip cut&paste to strip cut&paste in $\mathbf{R}^2$.

set when no singular points are present. For example, the flower normal form (FNF) of the cones of the points $\bar{p}_8, \bar{p}_9, \bar{p}_{10}, \bar{p}_{11}$, and $\bar{p}_{12}$ in Figure 2 are given by:

	Cone	FNF		Cone	FNF		Cone	FNF
$\bar{p}_8$			$\bar{p}_9$			$\bar{p}_{11}$		
$\bar{p}_{12}$			$\bar{p}_{10}$					

4.3 The transformations for regular semi-algebraic sets in $\mathbf{R}^3$

For regular semi-algebraic sets in $\mathbf{R}^3$, we introduce the following transformations:

- **Cylindrical replacement**, which enables to replace isolated sets of the form $A' \times [0,1]$ by $B' \times [0,1]$ if A' is $\mathcal{I}_2$-equivalent to B'.
- $3d$**-tube cut&paste and complement** $3d$**-tube cut&paste**, three-dimensional counterparts of the two-dimensional strip cut&paste transformations. These transformations are shown in Figure 6.
- **Wire cut&paste**, which does not have a two-dimensional counterpart. It allows to rewire wires that have the same profile, as shown in Figure 7.
- **Unknotting wires**, which allows to unentangle wires, possibly of different profiles, as shown in Figure 9.
- **Local cone surgery**, which allows to replace a cone of a point by a topologically elementary equivalent cone. It does so by applying strip cut&paste transformations directly on the cones of points, rather than on their stereographic projections, as shown in Figure 11.

In the remainder of this section, we discuss these transformations in more detail and show that they indeed preserve $\mathcal{I}_3$-equivalence.

4.4 Cylindrical replacement

We start by showing that in a semi-algebraic set A in $\mathbf{R}^3$ one can replace any isolated cylindrical set $A' \times [0,1]$ in the working cube I^3 by another cylindrical set $B' \times [0,1]$, provided that A' and B' are two-dimensional sets, located in the interior of the working square $I^3_{z=0}$, that are $\mathcal{I}_2$-equivalent. If we denote the resulting set by B, than A is $\mathcal{I}_3$-equivalent to B. It is a transformation that directly "lifts" topological elementary equivalence in $\mathbf{R}^2$ to $\mathbf{R}^3$.

Proposition 4.1 *If A and B are two regular sets in $\mathbf{R}^3$ that differ in the working cube I^3 by $A' \times [0,1]$ versus $B' \times [0,1]$, where A' and B' are two-dimensional sets in the working square $I^3_{z=0}$ that are $\mathcal{I}_2$-equivalent and if $\partial I^3 \cap A = \emptyset$ and $\partial I^3 \cap B = \emptyset$, then A and B are $\mathcal{I}_3$-equivalent.*

P r o o f. Let A and B be as described in the statement of the proposition. We argue that if there is a topological sentence φ^3 that distinguishes between A and B (that is, $A \models \varphi^3$ and $B \not\models \varphi^3$), then there is also a topological sentence φ^2 that distinguishes between A' and B'. This would give a contradiction. Let S be a binary relation symbol representing sets in $\mathbf{R}^2$. We describe how $\varphi^2(S)$ is constructed. First, we scale and translate S into $s(S)$ to fit in the working square I^2 (without touching its borders). Next, we construct $s(S) \times [0,1]$ and we set $D(S) := s(S) \times [0,1] \cup (A \cap (\mathbf{R}^3 \setminus I^3))$. It is clear that $D(S)$ is first-order constructible in the language of the alphabet $(0, 1, +, \times, <, S)$. We also remark that $A \cap (\mathbf{R}^3 \setminus I^3)$, the part of A outside the working cube I^3, equals $B \cap (\mathbf{R}^3 \setminus I^3)$, by assumption. We can then use φ^3 to distinguish between A' and B'. Indeed, $D(A') \models \varphi^3$ and $D(B') \not\models \varphi^3$. It remains to be shown that this construction is invariant under isotopies of the plane.

Let A'_1 and A'_2 be sets in $\mathbf{R}^2$ such that there is an isotopy $i : \mathbf{R}^2 \to \mathbf{R}^2$ with $i(A'_1) = A'_2$. Then it is clear that $s(A'_1) \times [0,1]$ and $s(A'_2) \times [0,1]$ are isotopic in $\mathbf{R}^3$ and the same holds for $s(A'_1) \times [0,1] \cup (A \cap (\mathbf{R}^3 \setminus I^3))$ and $s(A'_2) \times [0,1] \cup (A \cap (\mathbf{R}^3 \setminus I^3))$. This shows that $\varphi^2(S) := \varphi^3(s(S) \times [0,1] \cup (A \cap (\mathbf{R}^3 \setminus I^3)))$ is an $\mathcal{I}_2$-invariant sentence and $A' \models \varphi^2$ whereas $B' \not\models \varphi^2$. This completes the proof. □

4.5 $3d$-tube cut&paste and complement $3d$-tube cut&paste

A $3d$-*tube* is a part of a semi-algebraic set that is (locally in some region) isotopic to a full cylinder (that is, $S^2(\bar{p}, r) \times (0,1)$). The transformation rules that we discuss in this paragraph are the $3d$-*tube cut* and its inverse, the $3d$-*tube paste*. We also discuss the complement versions of these transformations. The $3d$-tube cut&paste transformations are the three-dimensional counterparts of the strip cut&paste transformations described earlier and are illustrated in Figure 6 (top). More formally, let A be a regular semi-algebraic in $\mathbf{R}^3$. Suppose that within the working cube I^3 the set A is a $3d$-tube (see Figure 6 (top, left)). Replacing $I^3 \cap A$ by a *cut* $3d$-tube (see Figure 6 (top, right)) is an application of the $3d$-*tube cut* transformation. Its inverse is the $3d$-*tube paste*.

Proposition 4.2 *Let A and B be regular semi-algebraic sets in $\mathbf{R}^3$. If B is obtained from A by a $3d$-tube cut or a $3d$-tube paste transformation, then A and B are $\mathcal{I}_3$-equivalent.*

P r o o f. We first consider a "weak" version of the $3d$-tube cut&paste transformations, in which a hole appears in one of the cut tube ends (like in the two-dimensional case, illustrated in Figure 3 (a)). To show that two sets A and B in $\mathbf{R}^3$, that differ a weak $3d$-tube cut or $3d$-tube paste from each other, are $\mathcal{I}_3$-equivalent, we imitate the proof of the two-dimensional weak strip cut&paste transformations, that uses a reduction to the inexpressibility of the problem MAJORITY(R_1, R_2) for two given finite sets R_1 and R_2 (see Section 4.1). As in $\mathbf{R}^2$, we place the finite sets R_1 and R_2 in a rectangular area J^2 in the working square $I^3_{z=0}$ of I^3, and perform the same construction $D(R_1, R_2)$, which we now "multiply" with $[0,1]$ to obtain tubes rather than strips. Next, we add to this the part of A (or B) outside I^3, making sure that the $3d$-tubes fit on the border of I^3. The argumentation is now the same: if there is an $\mathcal{I}_3$-invariant sentence that can distinguish between A and B that differ by a weak $3d$-tube cut&paste transformation from each other, then we obtain a first-order expression for MAJORITY(R_1, R_2), which gives a contradiction.

To go from the "weak" $3d$-tube cut&paste to the $3d$-tube cut&paste, we can again follow an argumentation from $\mathbf{R}^2$, which is already illustrated for the strip case in Figure 5. First, we perform a weak $3d$-tube cut which is a lifted version of (a) shown in Figure 5. Next, we double the isolated cube, using Proposition 4.1 (one filled

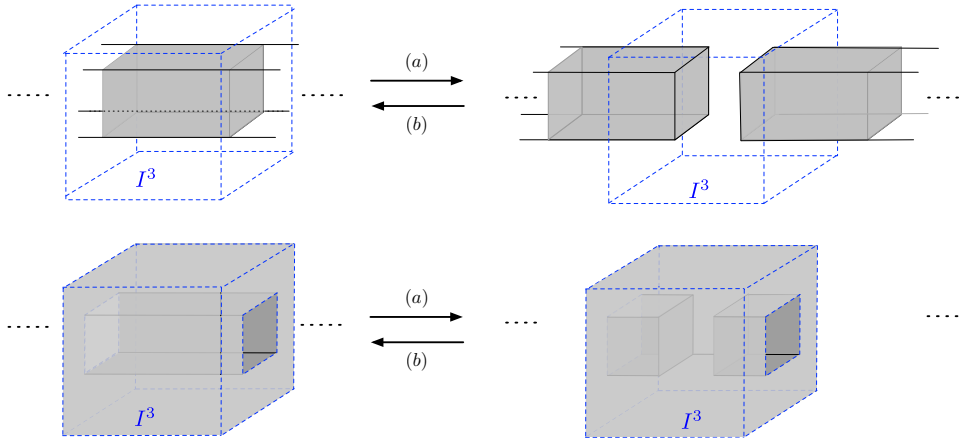

Fig. 6 Top: The $3d$-tube cut (a) and $3d$-tube paste (b). Bottom: The complement $3d$-tube cut (a) and complement $3d$-tube paste (b).

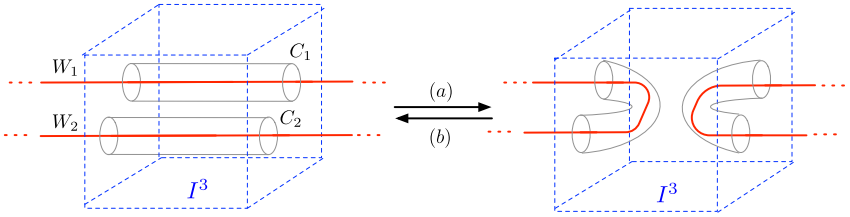

Fig. 7 The wire cut (a) and wire paste (b). The red lines represent wires of type k.

square and two filled squares are $\mathcal{I}_2$-equivalent). Finally, we perform three more weak $3d$-tube cut&pastes to obtain the $3d$-tube cut. This completes the proof. □

We also need a complement version of the $3d$-tube cut&paste transformations, referred to as the *complement $3d$-tube cut&paste* transformations, as is illustrated in Figure 6 (bottom). Here, inside the working cube I^3 the semi-algebraic set is isotopic to an empty cylinder (that is, $I^3 \setminus (S^2(\bar{p}, r) \times (0, 1))^\circ$) and the complement $3d$-tube cut transformation cuts this empty cylinder in two parts as shown in Figure 6 (bottom, right). The complement $3d$-tube paste transformation glues two empty cylinders together as shown in Figure 6 (bottom, left). The proof that this transformation preserves $\mathcal{I}^3$-equivalence is entirely analogous to the proof of Proposition 4.2. One only needs to complement the construction given there.

4.6 Wire cut&paste

Consider the working cube I^3 and two disjoint parallel cylinders C_1 and C_2 in I^3. If in a set A in $\mathbf{R}^3$, we have two wires W_1 and W_2 of the same profile k such that within C_1 (resp., C_2), W_1 (resp., W_2) is isotopic to $[0, 1] \times P_k$, where P_k is a $2d$-cone of type (R^k), and C_1 (resp., C_2) does not contain anything else than W_1 (resp., W_2), then these wires can be cut and rewired, as illustrated in Figure 7. We call this transformation, the *wire cut&paste*. This transformation is its own inverse. The following property shows that rewiring produces $\mathcal{I}_3$-equivalent sets.

Proposition 4.3 *Let A and B be regular semi-algebraic sets in $\mathbf{R}^3$. If B is obtained from A by a wire cut&paste transformation, then A and B are $\mathcal{I}_3$-equivalent.*

Proof. As before, we first consider a "weak" version of wire cut&paste. This transformation rewires two wires of the same profile with a wire loop of that profile as a side effect. Assume that the profile of the wires is k. To show that two sets A and B in $\mathbf{R}^3$, that differ a weak wire cut&paste from each other, are $\mathcal{I}_3$-equivalent, we again imitate the proof of the two-dimensional weak strip cut&paste, that uses a reduction to the inexpressibility

of the problem MAJORITY(R_1, R_2) for two given finite sets R_1 and R_2 (see Section 4.1). We assume that the wires of A (and B) enter the working cube I^3 in a "controlled" fashion, that is, they enter transversally the left and right face of I^3 and if we denote by $I^3_{x=-2}$ and $I^3_{x=2}$ the left- and right-hand face of I^3, then $A \cap I^3_{x=-2}$ consists of two disjoint cones both having as base k line segments on $I^3_{x=-2} \cap I^3_{z=-1}$ and as top a point on $I^3_{x=-2} \cap I^3_{z=0}$ (and similarly for $A \cap I^3_{x=2}$). We remark that this is possible because we assume these wires to be isotopic to $[0,1] \times P_k$, where P_k is a $2d$-cone of type (R^k).

As in $\mathbf{R}^2$, we place the finite sets R_1 and R_2 in a rectangular area J^2 in the working square $I^3_{z=0}$ and perform the same construction $D(R_1, R_2)$, of which, next, we take the topological border in order to obtain piecewise linear curves. We connect these to the tops of the cones in the intersection of A with the border of I^3. We recall that these tops also lie on $I^3_{z=0}$, as just explained. To conclude our construction, we turn the curves on $I^3_{z=0}$ into wires in I^3 of the correct profile, ensuring that they seamlessly connect to A (or B) on the border of I^3. This is done in three steps:

1. We first smoothen the corner points (where two line segments meet) in $D(R_1, R_2)$ by means of a simple Bézier-curve construction (expressible in first-order). Here, care is needed to ensure that the curves do not intersect with other line segments. This can be achieved by working locally around the corner points (e.g., within their cone radii).

2. Next, for each point $\bar{p}$ on these curves a vertical plane $V_{\bar{p}}$ orthogonal to the curve in $\bar{p}$ is considered. We note that this is possible because of the previous smoothing step. In the plane $V_{\bar{p}}$, we construct a cone with top $\bar{p}$ and base consisting of k disjoint line segments that lie on the intersection of $V_{\bar{p}}$ and $I^3_{z=-1}$. We do this for each point on the curves. Furthermore, we take the k line segments small enough so that no undesired intersections take place. For this purpose we identify a uniform cone radius, that is, a radius that is a cone radius for every point on the curves. It can be easily verified that such a uniform cone radius exists (see also [26]). The k line segments are then chosen such that they are covered by an interval of length smaller than the uniform cone radius. The result is that, within the cube $J^2 \times [-1, 0]$, we have wires of the desired profile.

3. As a final step, consider the left face $I^3_{x=-2}$ on which we have two cones, both with a base consisting of k line segments $[a_1, b_1], [a_2, b_2], \ldots, [a_k, b_k]$ on $I^3_{x=-2} \cap I^3_{z=-1}$. On the other hand, on the left face of $J^2 \times [-1, 0]$ we have also two cones that also have as base k line segments $[a'_1, b'_1], [a'_2, b'_2], \ldots, [a'_k, b'_k]$. To glue these together, we add cones with appropriately scaled bases in the plane $V_{\bar{p}}$, for each point $\bar{p}$ on the line segments connecting the points on the border of J^2 with tops of the cones on $I^3_{x=-2}$. We perform a similar construction for the right face $I^3_{x=2}$. As a result, we have wires of profile k inside I^3 that connect seamlessly with the intersection of A (or B) and the border of I^3.

Given that the uniform cone radius can be expressed in first-order logic (Lemma 5.5. in [26]), it should be clear that the entire construction can be expressed in first-order logic.

The argumentation is now the same: if there is an $\mathcal{I}_3$-invariant sentence that can distinguish between A and B that differ a weak wire cut&paste from each other, then we obtain a first-order expression of MAJORITY(R_1, R_2), which gives a contradiction.

To go from the "weak" wire cut&paste to the wire cut&paste, we follow the process illustrated in Figure 8. First, a weak wire cut is performed in the blue working cube (see Arrow (a) in Figure 8). This weak cut causes a wire loop of type k. Next (Arrow (b)), this wire loop can be replaced by two wire loops. To show that this preserves $\mathcal{I}_3$-invariance, a similar argumentation as the one used in Lemma 5 in [12] can be used, by means of a reduction to the first-order inexpressibility of PARITY(R). The decision problem PARITY(R) asks whether a finite set R has an even number of elements. Finally, Arrow (c) shows another application of the weak wire paste, eliminating the two wire loops. This completes the proof. □

4.7 Unknotting wires

The wires in a regular semi-algebraic set A in $\mathbf{R}^3$ can form *knots* and *links*. It is known in knot theory [27, 28] that each knot or link can be untangled by the *unknotting operation*. This transformation, illustrated in Figure 9, allows to change an overcrossing to an undercrossing. More precisely, consider the working cube I^3 and two

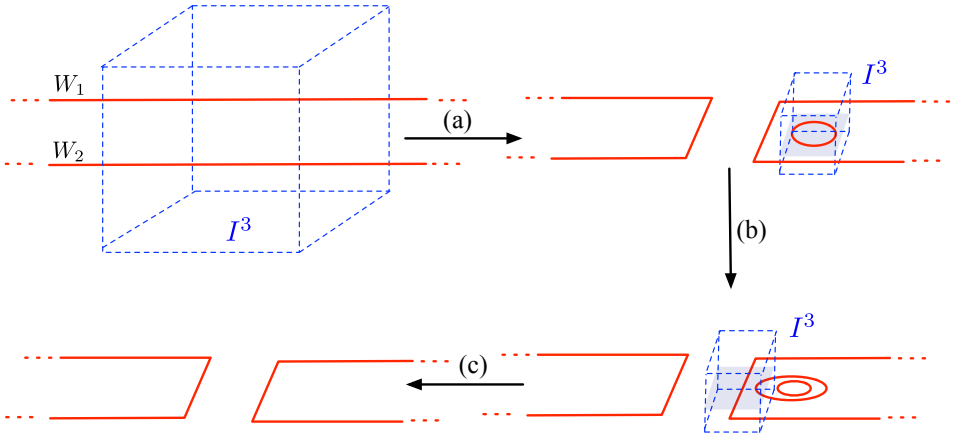

Fig. 8 The proof steps of going from weak wire cut&paste to wire cut&paste.

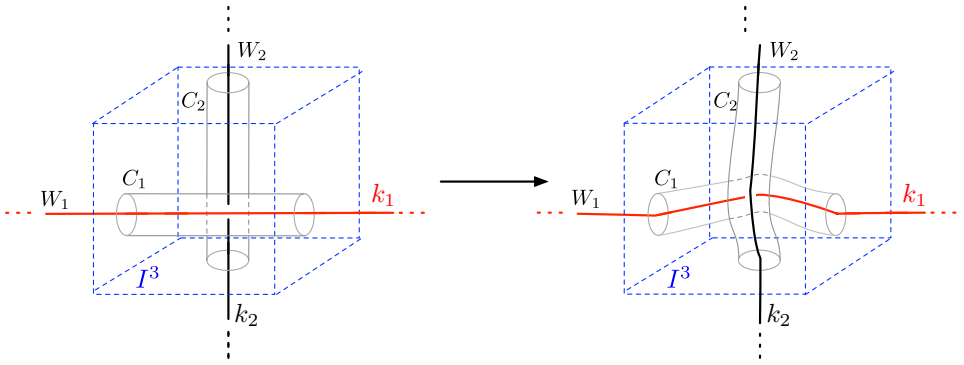

Fig. 9 The unknotting transformation. The red lines represent wires of profile k_1 and the black lines wires of profile k_2.

disjoint cylinders C_1 and C_2 in I^3 that "cross" each other, that is, C_1 is "above" C_2 when viewed from the front of I^3. Then, if in a set A we have two wires W_1 and W_2 of profile k_1 and k_2, respectively, such that within C_1 (resp., C_2), W_1 (resp., W_2) is isotopic to $[0,1] \times P_{k_1}$ (resp., $[0,1] \times P_{k_2}$), where P_{k_1} is a $2d$ cone of type (R^{k_1}), and similarly P_{k_2} is a $2d$ cone of type (R^{k_2}), and furthermore, C_1 (resp., C_2) does not contain anything else than W_1 (resp., W_2), then the *unknotting transformation* brings W_1 "below" W_2, as is illustrated in Figure 9. The following property shows that the unknotting transformation produces $\mathcal{I}_3$-equivalent sets.

Proposition 4.4 *Let A and B be regular semi-algebraic sets in $\mathbf{R}^3$. If B is obtained from A by an unknotting transformation, then A and B are $\mathcal{I}_3$-equivalent.*

Proof. Let us consider a wire of profile k_1 and a wire of profile k_2 in the working cube I^3, as described above. The proof argument is illustrated in Figure 10. First, the wire of profile k_1 is "bend around" the wire of profile k_2, followed by a wire cut&paste on the wire of profile k_1 (Arrow (a) in Figure 10). This results in the wire of profile k_1 moving from overcrossing to undercrossing the wire of profile k_2, at the cost of an extra wire loop of profile k_1 around the wire of profile k_2. Again, using a reduction to the first-order inexpressibility of PARITY(R) (see Lemma 5 in [12]), this loop can be doubled (see Arrow (b) in Figure 10). Finally, using the wire cut&paste, this double loop can be cut open into a single loop that is no longer around the wire of profile k_2 (see Arrow (c) in Figure 10). This loose loop can then be absorbed into the wire of profile k_1, again using the wire cut&paste transformation (see Arrow (d) in Figure 10). This completes the proof. □

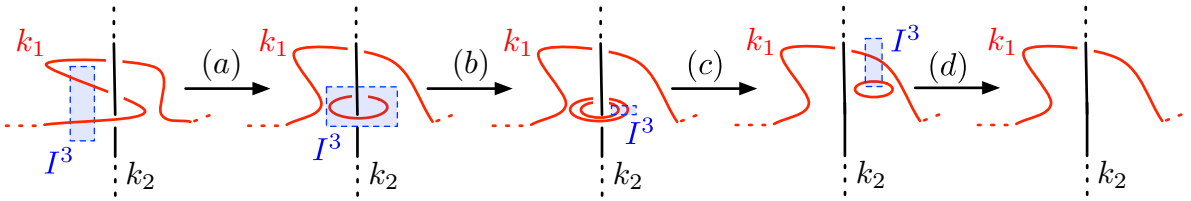

Fig. 10 The proof process for the unknotting transformation.

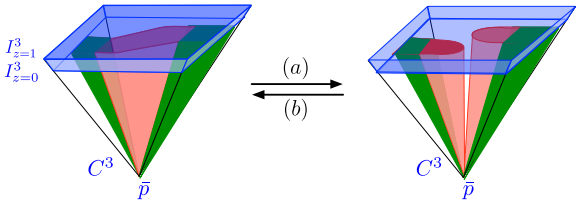

Fig. 11 Local cone surgery.

4.8 Local cone surgery

To conclude, we discuss a transformation that will allow us to bring cones of points into a canonical form. More precisely, local surgery around a point is a local application of the strip cut&paste transformation on the cone of that point. We have seen that in $\mathbf{R}^2$, every regular set can be brought into flower normal form (see Section 4.2), and local surgery enables us to transform cones in $\mathbf{R}^3$ (when viewed as sets in $\mathbf{R}^2$) into this normal form.

Figure 11 illustrates the situation we discuss here. Instead of the working cube I^3 we use working cone C^3 given by $\text{Cone}(I^3_{z=1}, \bar{p})$ for a point $\bar{p}$ under consideration. The cone of $\bar{p}$ in C^3 lies on the $I^3_{z=0}$ plane and as shown in the left part of Figure 11, within C^3 this cone consists of a strip (shown in red). Optionally, this strip can extend to the boundaries of C^3 (shown in green), and above the cone a filled area can be present (shown in blue). In the right part of Figure 11, the base of this cone is a cut strip (shown in red) whereas the optional green and blue parts are unchanged. Local surgery can be applied in both directions (Arrows (a) and (b) in Figure 11) and is thus indeed a "lifted" strip cut&paste transformation to the cone of a point in $\mathbf{R}^3$, rather than its stereographic projection.

To show that local surgery indeed preserves $\mathcal{I}_3$-equivalence, we need the following lemma.

Lemma 4.5 *If A and B are two regular sets in $\mathbf{R}^3$ that differ in the working cone C^3 by $\text{Cone}(A', \bar{p})$ versus $\text{Cone}(B', \bar{p})$, where A' and B' are $\mathcal{I}_2$-equivalent subsets of $I^3_{z=0}$ and if $\partial C^3 \cap A = \bar{p}$ and $\partial C^3 \cap B = \bar{p}$, then A and B are $\mathcal{I}_3$-equivalent.*

The proof of this lemma follows the same lines as the one of Proposition 4.1, with the modification that we use $\text{Cone}(s(S), \bar{p})$ instead of $s(S) \times [0, 1]$.

Lemma 4.5, when applied to the set A of Figure 2, shows that the two cones that touch in $\bar{p}_{12}$ can be replaced by a single cone, which in fact is just a closed ball (since one and two closed disks are indistinguishable in $\mathbf{R}^2$). This is precisely why $\bar{p}_{12}$ was called a fake $3d$-boundary point, that is, its cone is equivalent to that of a regular $3d$-boundary point.

We remark that the lemma also holds when, as depicted in Figure 11, a filled box resides above $\text{Cone}(A', \bar{p})$ versus $\text{Cone}(B', \bar{p})$ in C^3 (that is, when the blue part in Figure 11 is present). The proof is a simple extension of the proof of Lemma 4.5. With Lemma 4.5 in place, we next show that local surgery preserves $\mathcal{I}_3$-equivalence.

Proposition 4.6 *Let A and B be regular semi-algebraic sets in $\mathbf{R}^3$. If B is obtained from A by local cone surgery, then A and B are $\mathcal{I}_3$-equivalent.*

Proof. We first consider a "weak" version of local cone surgery, in which a hole appears in one of the cut conical ends. This is illustrated in Figure 12, where only the situation in the plane $z = 0$ is depicted. This figure

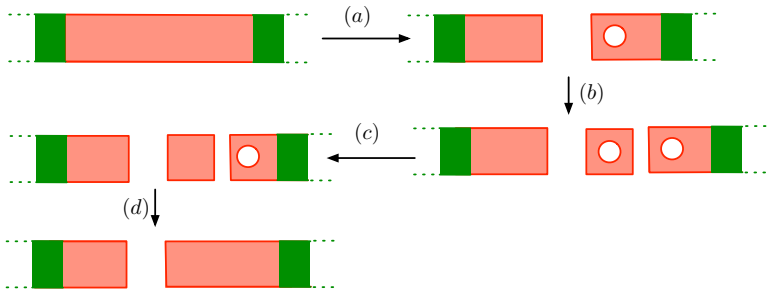

Fig. 12 The proof process for local cone surgery. Only the situation in the plane $z = 0$ is depicted here.

should be combined with Figure 11 to get a three-dimensional view. Weak local cone surgery is shown in (a) and to show that two sets A and B in $\mathbf{R}^3$, that differ by a weak local cone surgery from each other, are $\mathcal{I}_3$-equivalent, we again use a reduction to the inexpressibility of the problem MAJORITY(R_1, R_2) for two given finite sets R_1 and R_2 (see Section 4.1).

Arrow (b) in Figure 12 is another application of weak local cone surgery. Next, in Arrow (c), we apply Lemma 4.5 which when applied to an isolated cone, replaces it by a cone with an equivalent ($\mathcal{I}_2$-equivalent) base. We use it here to replace an annulus with a disk. Arrow (d) in Figure 12 is another application of weak local cone surgery. This completes the sketch of the proof. □

5 Transformation of regular semi-algebraic sets into their canonical form

In this section, we describe how an arbitrary regular semi-algebraic set in $\mathbf{R}^3$ can be transformed into a canonical form. We start by defining the canonical form for point structures.

5.1 The canonical form of point structures

We define the canonical form of a point structure in a number of stages, depending on what cone types occur in the point structure $\Pi_3(A)$ of a regular semi-algebraic set A in $\mathbf{R}^3$. If $\Pi_3(A)$ (and hence also A) is the empty set, then the canonical form of $\Pi_3(A)$ is the empty set in $\mathbf{R}^3$. Next, if $\Pi_3(A)$ is not empty but does not contain cone encodings of wire points, then we define the canonical form of $\Pi_3(A)$ to be the unit ball $B^3((0,0,0),1)$ in $\mathbf{R}^3$.

The more interesting case is when $\Pi_3(A)$ does contain cone encodings of wire points. To define its canonical form, we first represent $\Pi_3(A)$ by means of an undirected multigraph G, to encode the connectivity between cone encodings of $3d$-singular points by means of wires, and a set of profiles $\mathcal{P}$ of cone encodings of wire points, to encode knotted wires whose profiles do not occur in the cone encodings of $3d$-singular points. As we have observed in the proof of "the only-if" direction of Theorem 3.6, this is precisely the information needed to characterise $\Pi_3(A)$, with the addition of connectivity information between singular points. This connectivity information (stored in the edges in G) is added to enable the construction of a regular semi-algebraic set A_G in $\mathbf{R}^3$ from G, as will become clear shortly. We ensure that G and $\mathcal{P}$ are uniquely determined by $\Pi_3(A)$.

More specifically, given $\Pi_3(A)$, we define the undirected edge-labeled multi-graph $G = (V, E, \lambda)$ such that each vertex $v \in V$ corresponds to a cone encoding of a $3d$-singular point in $\Pi_3(A)$, and each edge $e = (v, w) \in E$, running between the singular points represented by v and w, represents a wire of profile $\lambda(e) \in \mathbf{N} \setminus \{0, 1\}$.

Clearly, the vertices in V can be easily inferred from $\Pi_3(A)$. As previously mentioned, $\Pi_3(A)$ does not store information as to which vertices are connected with each other by means of wires. Indeed, $\Pi_3(A)$ only indicates that there exists a regular semi-algebraic set (e.g., A) that has $\Pi_3(A)$ as point structure. Our aim, however, is to associate a semi-algebraic set A_G to G, by using the information in $\Pi_3(A)$ alone, such that $\Pi_3(A_G) = \Pi_3(A)$. Furthermore, A_G is uniquely determined by G (and hence also by $\Pi_3(A)$).

For this purpose, we define an ordering on the vertices in V. For example, suppose that v is a vertex that corresponds to the cone encoding $\{\!\{F^\infty, (R)^\infty, (R^{k_1})^{n_1}, \ldots, (R^{k_\ell})^{n_\ell}\}\!\}$ of a $3d$-singular point. We can associate a unique natural number to v, denoted by $\mathfrak{p}(v)$, and use these numbers to define an ordering on V. Indeed, let us

denote by p_i the ith prime number. Then we define $\mathfrak{p}(v) = p_{k_1}^{n_1} \cdots p_{k_\ell}^{n_\ell}$. In this way, each cone encoding can be associated with a unique number and we define $v \leq w$ if and only if $\mathfrak{p}(v) \leq \mathfrak{p}(w)$.

We next define the edges in G. Each edge represents a wire of certain profile and we need to ensure that the number of types of edges is consistent with the cone encodings corresponding to their adjacent vertices. Consider a vertex v that corresponds to the cone encoding $\{\!\{F^\infty, (R)^\infty, (R^{k_1})^{n_1}, \ldots, (R^{k_\ell})^{n_\ell}\}\!\}$ of a $3d$-singular point. We observe that $(R^{k_i})^2$ can be interpreted as a *single* wire of profile k_i that starts and ends in v. In general, $(R^{k_i})^{n_i}$ can be seen as m_i wires of profile k_i, where $n_i = 2m_i$ when n_i is even, and $n_i = 2m_i + 1$ when n_i is odd, such that each of these m_i wires starts and end in v. When n_i is odd, we need one more wire of profile k_i that starts in v and ends in another vertex w. As before, let v be a vertex that corresponds to the cone encoding $\{\!\{F^\infty, (R)^\infty, (R^{k_1})^{n_1}, \ldots, (R^{k_\ell})^{n_\ell}\}\!\}$. Based on this observation, we define E as follows:

(a) The multi-set E must contain $M = m_1 + \cdots + m_\ell$ distinct edges $e_i^j = (v, v)$ of profile $\lambda(e_i^j) = k_i$, for $1 \leq i \leq \ell$ and $1 \leq j \leq m_i$.

(b) Furthermore, v must be adjacent to $n_1 + \cdots + n_\ell - 2M$ other distinct edges $f_i^j = (v, w_i^j)$ in E, of profile $\lambda(f_i^j) = k_i$, and such that $v \neq w_i^j$, for $1 \leq i \leq \ell$ and $1 \leq j \leq n_i - m_i$.

These two conditions ensure that vertex v is adjacent to $n_1 + \cdots + n_\ell$ edges, each of which representing a wire occurring in the cone encoding of the $3d$-singular point corresponding to v.

To make the definition of E canonical, it remains to clarify which vertices w_i^j in Case (b) are selected. We define w_i^j as the smallest vertex in V, relative to the ordering defined previously, such that $v \leq w_i^j$ and w_i^j corresponds to a $3d$-singular point whose cone encoding has an odd number of cones of the form (R^{k_i}). In case that multiple such vertices exist, this implies that they all represent the same cone, and we can safely break ties arbitrarily. This concludes the definition of G.

We further have to account for cone encodings of knotted wires, that is, wires that are not attached to singular points. To this aim, let $\mathcal{P}$ be a finite set of natural numbers in $\mathbb{N} \setminus \{0, 1\}$, each element in $\mathcal{P}$ corresponding to the profile k_i of a wire, represented by an occurrence of $\{\!\{F^\infty, (R)^\infty, (R^{k_i})^2\}\!\}$ in $\Pi_2(A)$. Furthermore, $(R^{k_i})^2$ should not appear in $\Pi_3(A)$ as part of the cone encoding of a $3d$-singular point. Hence, each $k \in \mathcal{P}$ will correspond to the profile k of a wire point that is not represented already by edges in G.

Next, we define the canonical form of $\Pi_3(A)$, given G and $\mathcal{P}$. First, we turn G into a regular semi-algebraic set in $\mathbf{R}^3$, as follows. Let $\imath$ be a so-called *book embedding* of G in $\mathbf{R}^3$ [29]. More specifically, all vertices in V are embedded in the *spine* $\{(0, 0)\} \times \mathbf{R}^+$ of the book, in an equidistant manner, as shown in Figure 13 (a) for vertices v_1, v_2, v_3 and v_4, according to the order imposed on V.

Then, for each edge e in E we assign a different *page* in the book embedding. In Figure 13 (a), edge e_1 is embedded in the red page, e_2 in the blue page, e_3 in the green page and e_4 in the yellow page. Each of these pages are an angle of $360°/|E|$ apart from each other; are vertical; and we assume a canonical assignment of edges in E to each of these pages. The actual embedding $\imath(e)$ of e in a page is done by means of a semi-circle that connects the points $\imath(v)$ and $\imath(w)$, where $e = (v, w)$, as illustrated in Figure 13 (a). If e is a self-loop, such as for edge e_3 in Figure 13 (a), a circle is used instead. We omit the precise description of this embedding as it should be clear from the figure that this can indeed be done in a canonical way.

Next, we turn each semi-circle $\imath(e)$ into a wire of the correct profile, that is, a wire of profile $\lambda(e)$. This is done in two steps, we first put a small cylinder C around the spine of the book, as shown in Figure 13 (b). Next, we put the desired profile on each semi-circle $\imath(e)$ up the boundary of the cylinder C. More specifically, for a wire of profile k, we put a flower with k petals on each point on the semi-circle, and this in a plane perpendicular to that point. This is illustrated in Figure 13 (b), where $\imath(e_1)$ and $\imath(e_3)$ have profile $k = 2$, and $\imath(e_2)$ and $\imath(e_4)$ have profile $k = 3$. Clearly, by constructing these profiles small enough compared to the positions of the pages of the book, one can easily ensure that these profiles do not intersect with each other. We denote by W_e the (partial) wire for e constructed in this way.

Finally, we connect the intersection of the partial wires and the cylinder C with their respective points on the book's spine, as shown in Figure 13 (c). More specifically, for each $v \in V$ we construct a cones with top $\imath(v)$ and base one of the two intersections of $W_e \cap C$, and this for each $e \in E$ adjacent to v. Clearly, these cones seamlessly complete the partial wires into wires that run between two (not necessarily distinct) points on the spine.

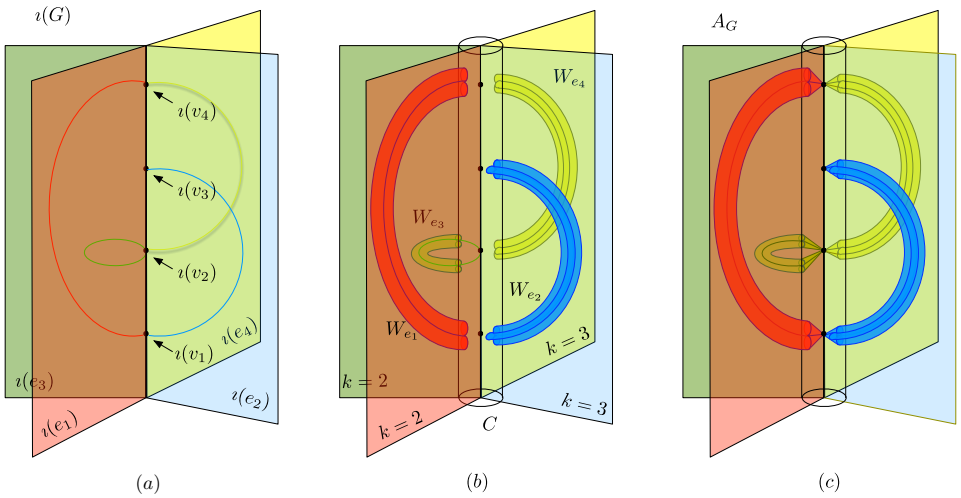

Fig. 13 Canonical form based on book embeddings in $\mathbf{R}^3$ of graphs.

Given $G = (V, E, \lambda)$ we denote by A_G the regular semi-algebraic set obtained in this way.

We next construct from $\mathcal{P}$ a regular semi-algebraic set in $\mathbf{R}^3$, as follows. Suppose that $\mathcal{P} = \{k_1, \ldots, k_n\}$, that is, $\mathcal{P}$ contains n distinct profiles of wires. Consider n horizontal planes $H_1, \ldots, H_n$ that are equally spaced out along the z-dimension and all having negative z coordinates. The latter ensures that these planes do not intersect with A_G (we recall that the spine of the book embedding has positive z coordinates). Next, we embed the unit circle $S^1((0,0),1)$ in each of the planes, and for each $k_i \in \mathcal{P}$, we turn the circle in H_i into a wire of profile k_i in a similar way as described earlier. We again ensure that none of these wires intersect with each other. We denote by $A_{\mathcal{P}}$ the regular semi-algebraic set obtained in this way, that is, it is a collection of n knotted wires that form individual loops.

To conclude, if $\Pi_3(A)$ has wire points, then we define its canonical form as $A_G \cup A_{\mathcal{P}}$. We note that $\Pi_3(A_G \cup A_{\mathcal{P}}) = \Pi_3(A)$, as desired. We now say that a regular semi-algebraic set A in $\mathbf{R}^3$ is in canonical form if it is the canonical form $A_G \cup A_{\mathcal{P}}$ of $\Pi_3(A)$.

5.2 Transformation process

Next, we show that a regular semi-algebraic set A in $\mathbf{R}^3$ can be transformed into a regular semi-algebraic set in canonical form by means isotopies and the $\mathcal{I}_3$-preserving transformations of Section 4. We start from a regular and compact semi-algebraic set A in $\mathbf{R}^3$ and let $\mathcal{Z}$ be a Whitney stratification of A. For a given point $\bar{p}$ of A, we denote by Z the unique stratum in $\mathcal{Z}$ to which $\bar{p}$ belongs.

The transformation process consists of the following five steps.

5.2.1 Step 1. Local surgery.

We first deal with points $\bar{p}$ for which $\dim(Z) = 0$ and that correspond to fake $3d$-boundary points, or $3d$-singular points. More specifically, by applying a number of local surgery transformations on A, resulting in a regular semi-algebraic set A_1, we ensure that for some $\varepsilon > 0$, $\sigma_2(A_1 \cap S^2(\bar{p}, \varepsilon))$ is in flower normal form, for these points, as defined in Section 4.2. Similarly, when $\bar{p}$ is a fake wire point, we apply local surgery transformations to turn this point into a proper wire point.

To identify which local surgery transformations we need to apply for fake $3d$-boundary points or $3d$-singular points, we recall that from the characterisation of $\mathcal{I}_2$-equivalence, we know that when $\varepsilon > 0$ is a cone radius of $\bar{p}$ in A, then $\sigma_2(A \cap S^2(\bar{p}, \varepsilon))$ can be transformed by means of number of strip cut&paste transformations into flower normal form. For fake wire points, $\sigma_2(A \cap S^2(\bar{p}, \varepsilon))$ is $\mathcal{I}_2$-equivalent to two $2d$-singular points that are connected by means of k filled regions, that is, the cone of a wire point of profile k. This implies again the existence of a sequence of strip cut&paste transformations that transform $\sigma_2(A \cap S^2(\bar{p}, \varepsilon))$ into the cone of a wire point.

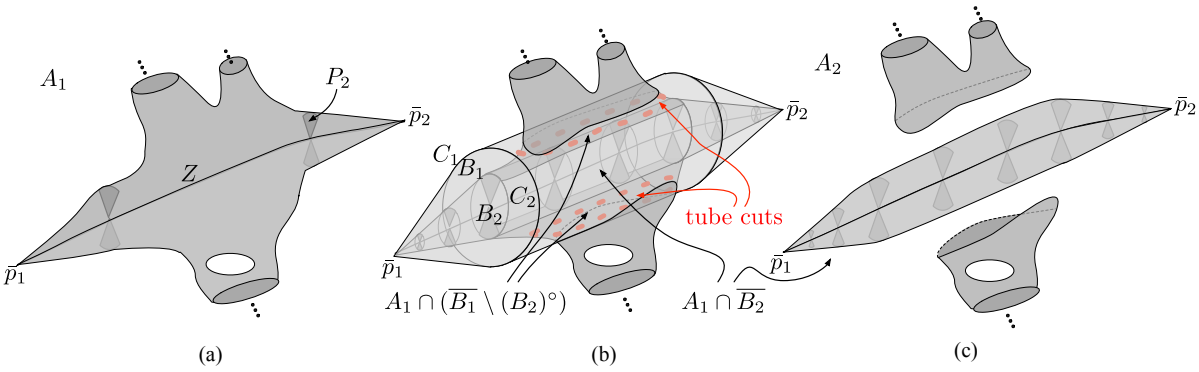

Fig. 14 Illustration of wire normalisation.

We can now use the *local surgery* transformation to simulate these sequences of strip cut&paste transformations on the actual cones, that is, on $A \cap S^2(\bar{p}, \varepsilon)$. In this way, A can be transformed into a set A_1, in an $\mathcal{I}_3$-equivalent way (by Proposition 4.6), such that

- fake $3d$-boundary points $\bar{p}$ in A are eliminated. Indeed, in A_1 we have that $\sigma_2(A_1 \cap S^2(\bar{p}, \varepsilon))$ is a single disk, that is, the cone type of a regular $3d$-boundary point;
- fake wire points $\bar{p}$ in A are eliminated. Indeed, in A_1 we have that $\sigma_2(A_1 \cap S^2(\bar{p}, \varepsilon))$ consists of two $2d$-singular points that are connected by means of k filled regions, that is, the cone type of a wire point; and
- $\sigma_2(A_1 \cap S^2(\bar{p}, \varepsilon))$ is a flower normal form for every $3d$-singular point $\bar{p}$.

One can further ensure that local surgery transforms the stratification $\mathcal{Z}$ of A into a Whitney-stratification $\mathcal{Z}_1$ of A_1 such that the zero-dimensional strata in $\mathcal{Z}_1$ do neither include fake $3d$-boundary points nor fake wire points. Furthermore, local surgery does not introduce new $3d$-singular points.

5.2.2 Step 2. Wire normalisation.

We next consider points $\bar{p}$ for which $\dim(Z) = 1$, for a Z in $\mathcal{Z}_1$, and that correspond to wire points of a certain profile k. We assume that Z is a smooth curve in $\mathbf{R}^3$, which we refer to as the *backbone* of the wire. We distinguish between the following cases: (a) Z ends in two distinct (necessarily) $3d$-singular points; (b) Z ends in the same $3d$-singular point; or (c) Z forms a knot. We note that these three cases are exhaustive since the previous step eliminated fake wire points and hence we may assume that the zero-dimensional strata adjacent to Z, if any, correspond to $3d$-singular points. We first consider Cases (a) and (b).

We want to "isolate" wires such that they resemble wires in sets in canonical form. More specifically, we argue that we only need to apply some isotopies to A_1 and k $3d$-tube cuts in order to obtain a regular semi-algebraic set A_2, such that the topological boundary of the $3d$-regular part of the wire is only adjacent to Z and its adjacent $3d$-singular points.

Figure 14 illustrates our intention: In Figure 14 (a), we show a wire of profile $k = 2$ that runs between two points $\bar{p}_1$ and $\bar{p}_2$ and whose $3d$-regular part may connect to other parts of A_1, as depicted by the dots. By contrast, in Figure 14 (c), we show the desired resulting set A_2. Here, the wire is detached and can be regarded as the product of Z with a flower consisting of two petals.

We next describe the transformation process for wires of profile k. First, we construct two "pinched" cylinders C_1 and C_2, locally around Z, such that both of them end in the $3d$-singular endpoints $\bar{p}_1$ and $\bar{p}_2$ of Z (see Figure 14 (b)). We distinguish between the inside and outside region defined by C_1 and C_2, in the usual way. Let B_1 be the inside region of C_1 and B_2 the inside region of C_2. By applying isotopies to A_1 and choosing C_1 and C_2 small enough, we can ensure that

- C_2 lies entirely inside $B_1 \cup \{\bar{p}_1, \bar{p}_2\}$;
- $A_1 \cap \overline{B_2}$ is isotopic to $Z \times P_k$, where $P_k \subseteq \mathbf{R}^2$ is a flower with k petals; and

- $A_1 \cap (\overline{B_1} \setminus (B_2)^\circ)$ is isotopic to k disjoint balls in $\mathbf{R}^3$.

In other words, $A_1 \cap \overline{B_2}$ is only adjacent with other $3d$-regular parts of A_1 by means of the k balls in $A_1 \cap (\overline{B_1} \setminus (B_2)^\circ)$. It now suffices to cut these k balls by means of $3d$-tube cut transformations to obtain the desired set A_2.

For Case (c), we reduce it to Case (b) by introducing a temporary fake wire point that serves as the endpoint of the backbone and then proceed as in Case (b), followed by the removal of the previously introduced fake wire point, using local surgery.

We denote by A_2 the regular semi-algebraic set obtained after normalising all wires in A_1 and denote by $\mathcal{Z}_2$ a stratification of A_2.

5.2.3 Step 3. Cleaning up the three-dimensional parts.

Let D be the three-dimensional regular part of A_2 that is not connected to wires. The boundary ∂D of D consists of surfaces (two-dimensional manifolds without boundary) embedded in $\mathbf{R}^3$. We note that ∂D may consist of multiple connected components, e.g., when D consists of multiple connected components itself or when D is homeomorphic to ball with a hole inside. We show that, using a representation of the embedding of D in $\mathbf{R}^3$, based on Morse theory [30], that D is topologically elementary equivalent to a ball in $\mathbf{R}^3$.

We start by describing this representation of ∂D and then indicate how to modify this into a representation of D.Without loss of generality we may assume that the surfaces constituting ∂D are smooth (that is, C^∞ manifolds). Furthermore, we may also assume that the height function $h : \mathbf{R}^3 \mapsto \mathbf{R}$ mapping (x, y, z) to $h(x, y, z) = z$ is a Morse function. Indeed, this can always be assumed by slightly perturbing ∂D [31]. Then, it is shown in [30] that the embedding of ∂D in $\mathbf{R}^3$ can be described, up to isotopy, as follows. Denote by Γ_v the set in $\mathbf{R}^3$ defined by $h^{-1}(v) = \{(x, y, z) \in \partial D \mid z = v\}$. Although Γ_v is a set in $\mathbf{R}^3$, it is often regarded as the set in $\mathbf{R}^2$ given by $\{(x, y) \in \mathbf{R}^2 \mid (x, y, z) \in \partial D, z = v)\}$. From the properties of Morse functions, it then follows that for all values $v \in \mathbf{R}$, except for a finite number of (so-called critical) values, Γ_v is a set consisting of embeddings of circles in $\mathbf{R}^2$. Furthermore, for any two consecutive critical values v_1 and v_2, Γ_v is isotopic to $\Gamma_{v'}$ for all v and v' such that $v_1 < v < v' < v_2$. Finally, locally around each critical value v and for small enough $\varepsilon > 0$, the change in topology between $\Gamma_{v-\varepsilon}$ and $\Gamma_{v+\varepsilon}$ can be described by considering a finite number of cases, as we explain below.

When applied to our setting, recall that we are considering a three-dimensional part D of A. As a consequence, we do not only have to consider ∂D but also the interior D° of D. We can, however, still describe the embedding of D in $\mathbf{R}^3$, up to isotopy, by means of the height function as just explained and as reported in [30].

Indeed, it suffices to take into account that Γ_v, which is now the inverse image of D under h at height v, is a $2d$-regular set rather than a union of embedded circles when only ∂D was concerned. Furthermore, when considering the local topological changes around critical values, the case analysis now also depends on which side of the boundaries the interior of D lies. We describe these cases in more detail below.

First, we explain how this representation of the embedding of D in $\mathbf{R}^3$ will be used to show that D that $\mathcal{I}_3$-equivalent to a ball in $\mathbf{R}^3$:

(A) For any two consecutive critical values v_1 and v_2, $v_1 < v_2$, we take a small $\varepsilon > 0$ and first detach $\{(x, y, z) \in \mathbf{R}^3 \mid (x, y) \in \Gamma_z, v_1 + \varepsilon \leqslant z \leqslant v_2 - \varepsilon\}$ from the rest of D by means of complement $3d$-tube paste transformations (see the lower part of Figure 6 for this transformation). We then show that each of these detached parts is $\mathcal{I}_3$-equivalent to a ball in $\mathbf{R}^3$, and that this ball can be merged with other $3d$-regular parts residing in a neighbourhood of Γ_{v_1} or Γ_{v_2}, using the $3d$-tube paste transformation.

(B) Locally around each critical value v, we inspect $\{(x, y, z) \in \mathbf{R}^3 \mid (x, y) \in \Gamma_z, v - \varepsilon \leqslant z \leqslant v + \varepsilon\}$. We have already hinted that only a finite number of local topological changes around a critical value can occur. We inspect each of these cases and show that we can again transform these sets into a union of balls in $\mathbf{R}^3$ by means of $3d$-tube cut&paste transformations. Hence, these parts of D are $\mathcal{I}_3$-equivalent to a union of balls in $\mathbf{R}^3$.

(C) Finally, we merge all balls into a single ball by means of the $3d$-tube paste transformation, showing that D is indeed $\mathcal{I}_3$-equivalent to a single ball in $\mathbf{R}^3$.

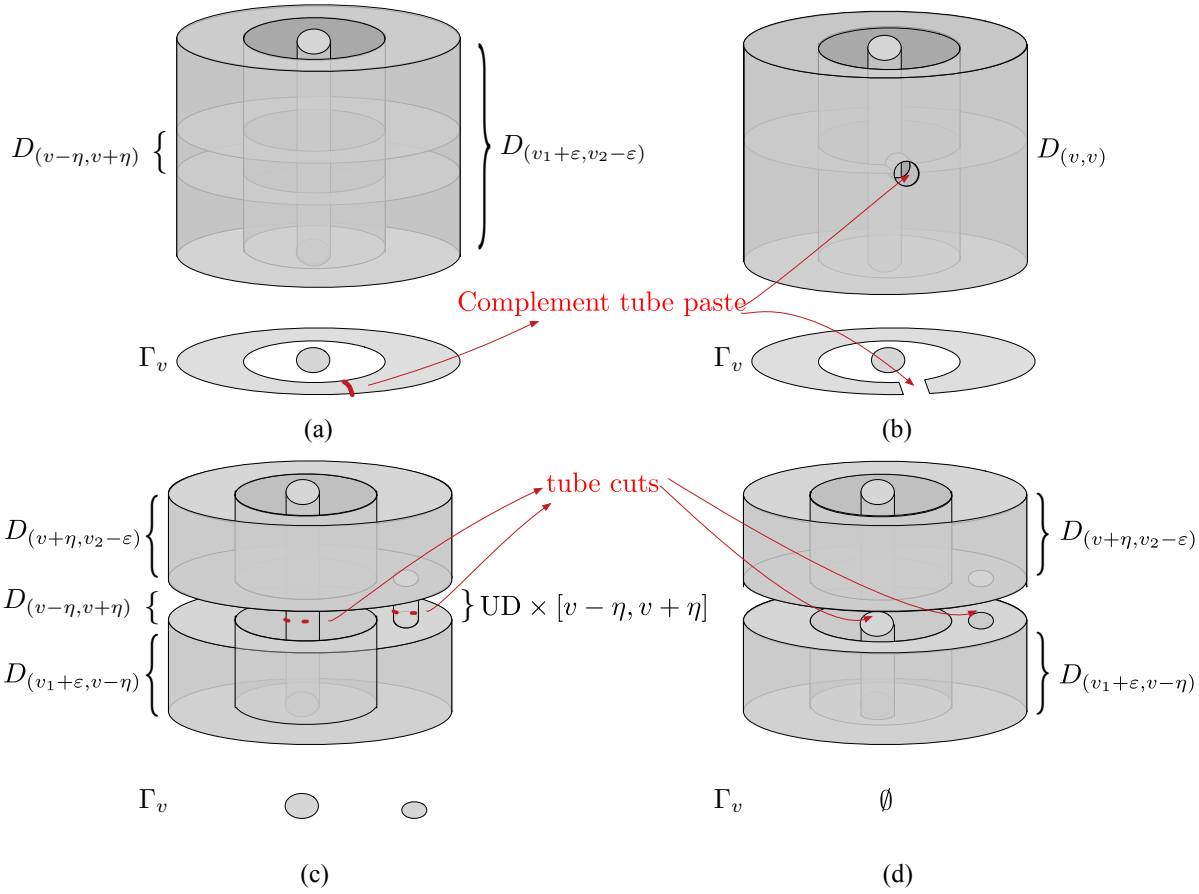

Fig. 15 Illustration of the detachment process between critical values.

In other words, we use the Morse function-based representation of the embedding of D in $\mathbf{R}^3$ to locally transform D into balls, hereby only inspecting a finite number of cases. This local approach avoids the need to deal with the possible complex manner in which D is globally embedded in $\mathbf{R}^3$. We next describe Steps A and B in more detail. Step C is an obvious application of $3d$-tube paste transformations and does not need further explanation.

Step A. Detachment between critical values. We describe how to detach $D_{(v_1+\varepsilon,v_2-\varepsilon)} = \{(x,y,z) \in \mathbf{R}^3 \mid (x,y) \in \Gamma_z, v_1+\varepsilon \leqslant z \leqslant v_2-\varepsilon\}$ from the rest of D just *above* the critical value v_1. How the set is detached just *below* v_2 is completely analogous.

In Figure 15, we illustrate the detaching process. We take a value v just above $v_1+\varepsilon$ and consider Γ_v, viewed as a $2d$-regular set in $\mathbf{R}^2$, as shown in the lower part of Figure 15 (a). To make the distinction clear, $D_{(v,v)}$ will denote Γ_v when viewed as a set in $\mathbf{R}^3$. We will detach $D_{(v_1+\varepsilon,v_2-\varepsilon)}$ around $D_{(v,v)}$. We note that we may assume that for small enough $\eta > 0$, $D_{(v-\eta,v+\eta)}$ is isotopic to $\Gamma_v \times [v-\eta, v+\eta]$, as shown in Figure 15 (a).

In $D_{(v,v)}$, we identify several paths (as will be explained in more detail shortly), that when complement $3d$-tube paste transformations are applied to $D_{(v-\eta,v+\eta)}$ along these paths, $D_{(v-\eta,v+\eta)}$ is isotopic to UD$\times[v-\eta, v+\eta]$, where UD is a union of, say k, disjoint disks in $\mathbf{R}^2$. In this way, $D_{(v_1+\varepsilon,v_2-\varepsilon)}$ is shown to be $\mathcal{I}_3$-equivalent to $D_{(v_1+\varepsilon,v-\eta)} \cup (\text{UD} \times [v-\eta, v+\eta]) \cup D_{(v+\eta,v_2-\varepsilon)}$.

In Figure 15 (a), we have identified a single path in $D_{(v,v)}$. For illustrative purposes, this path is shown in red in Γ_v in the lower part in Figure 15 (a). The result after applying a complement $3d$-tube paste to $D_{(v,v)}$, along this curve is shown in Figure 15 (b). We observe that Γ_v has indeed become isotopic to two disks.

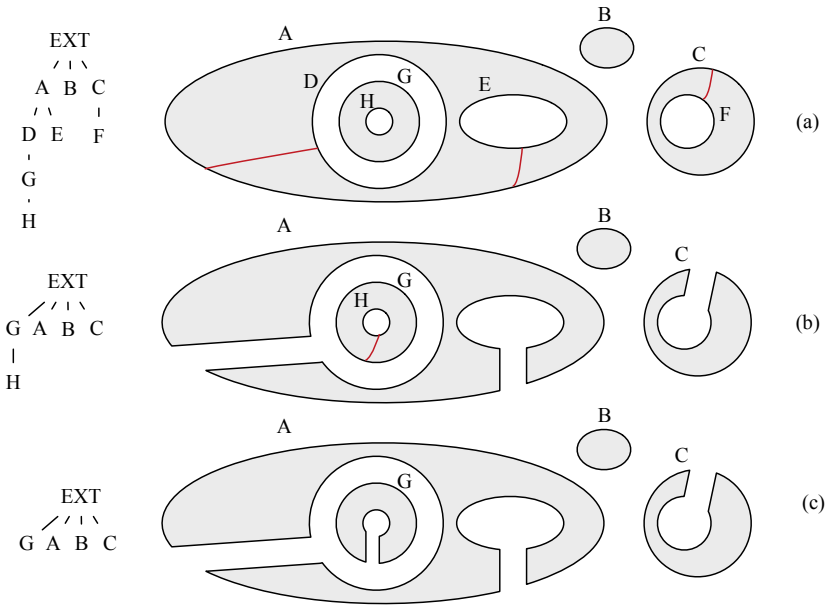

Fig. 16 Tree representations of Γ_v. Capital letters denote the embedded circles. Furthermore, (a) represents Γ_v, (b) represents Γ_v after connecting holes at depth 2 with EXT, (c) represents Γ_v after further connecting holes at depth 4 with EXT. Moreover, (c) is homeomorphic to a union of disjoint disks.

In Figure 15 (c), we have deformed $D_{(v-\eta,v+\eta)}$ such that it is isotopic two cylinders, one cylinder for each of the two disks in Γ_v. Next, we apply $3d$-tube cut transformations to each of the k cylinders in UD $\times\, [v-\eta, v+\eta]$, as shown in Figure 15 (d) for two cylinders. As a consequence, $D_{(v_1+\varepsilon,v_2-\varepsilon)}$ is $\mathcal{I}_3$-equivalent to $D_{(v_1+\varepsilon,v-\eta)} \cup D_{(v+\eta,v_2-\varepsilon)}$. We observe that in the latter set, $\Gamma_{v'} = \emptyset$ for $v' \in (v-\eta, v+\eta)$ and hence we indeed detached a part of $D_{(v_1+\varepsilon,v_2-\varepsilon)}$ around Γ_v. In a similar way, we can detach $D_{(v_1+\varepsilon,v_2-\varepsilon)}$ around a value w just below $v_2-\varepsilon$. We may thus conclude that $D_{(v_1+\varepsilon,v_2-\varepsilon)}$ is $\mathcal{I}_3$-equivalent to the union of three disjoint pieces, $D_{(v_1+\varepsilon,v-\eta)}$, $D_{(v+\eta,w-\eta)}$, and $D_{(w+\eta,v_2-\varepsilon)}$.

Let us first consider $D_{(v+\eta,w-\eta)}$. Clearly, it is isotopic to $\Gamma_u \times [0,1]$, for some $u \in (v+\eta, w-\eta)$. Since Γ_u is $\mathcal{I}_2$-equivalent to a single disk (any non-empty $2d$-regular set with no $2d$-singular points is $\mathcal{I}_2$-equivalent to a single disk) and $D_{(v+\eta,w-\eta)}$ is detached from anything else, Lemma 4.1 applies. We may thus conclude that $D_{(v_1+\varepsilon,v_2-\varepsilon)}$ is $\mathcal{I}_3$-equivalent to $D_{(v_1+\varepsilon,v-\eta)} \cup C \cup D_{(w+\eta,v_2-\varepsilon)}$ for an isolated cylinder C in $\mathbf{R}^3$. However, this cylinder can be removed. Indeed, since $D_{(v_1+\varepsilon,v-\eta)}$ contains some $3d$-regular parts, we apply a $3d$-tube paste transformation, connecting C with $D_{(v_1+\varepsilon,v-\eta)}$. As a result, C is absorbed into $D_{(v_1+\varepsilon,v-\eta)}$. In other words, we have eliminated $D_{(v+\eta,w-\eta)}$ from $D_{(v_1+\varepsilon,v_2-\varepsilon)}$. The remaining parts, $D_{(v_1+\varepsilon,v-\eta)}$ and $D_{(w+\eta,v_2-\varepsilon)}$ will be dealt with when considering the critical values v_1 and v_2.

Before considering the transformation process around critical values, it remains to explain which complement $3d$-tube paste transformations are applied to $D_{(v-\eta,v+\eta)}$ to make this set $\mathcal{I}_3$-equivalent to a union of cylinders. In view of the assumption that $D_{(v-\eta,v+\eta)}$ is isotopic to $\Gamma_v \times [v-\eta, v+\eta]$, we describe the process by considering the effect of these transformations on Γ_v, as shown in Figures 16 (a)–(c). First, we observe that Γ_v can be represented as a tree in which each node (apart from the root node) corresponds to an embedding of a circle in $\mathbf{R}^2$; the root node (at depth 0) corresponds to the exterior EXT of Γ_v; nodes at an odd depth indicate that the inside of the corresponding embedded circle is "full", that is, consists of $2d$-regular points; whereas nodes at an even depth indicate that the outside of the corresponding circle is full.[5] Furthermore, for a node at odd (resp., even) depth, children indicate holes (resp., filled regions) in the full (resp., empty) region corresponding to the parent node. We have illustrated this tree representation in Figures 16 (a)–(c).

More specifically, in these figures, we depict how we can recursively transform Γ_v into a number of disjoint disks. Starting from Figure 16 (a), we identify simple paths from the embedded circles at Level 1 in the tree

[5] The notion of inside and outside of an embedded circle in $\mathbf{R}^2$ are defined as usual [23].

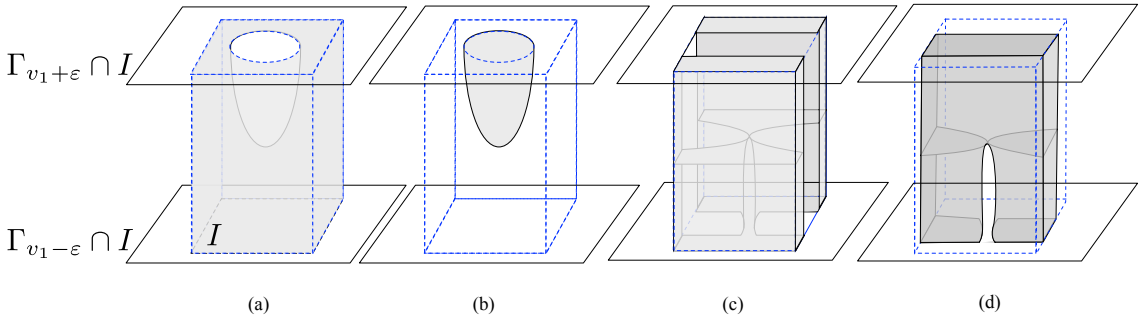

Fig. 17 Local topological changes around a critical value v_1. Inside I, $\Gamma_{v_1+\varepsilon}$ differs from $\Gamma_{v_1-\varepsilon}$ by the removal of an empty region (a), the removal of a filled region (b), the splitting of an empty region in two parts (c), or the splitting of filled region in two parts (d).

representation (A, B, and C) to their children, if any. In the figure we have shown the paths from A to D, A to E and C to F in red. We then "drill" small tunnels in $D_{(v-\eta,v+\eta)}$, as explained earlier, following these red paths by means of the complement $3d$-tube paste transformation. The result is a set that is $\mathcal{I}_3$-equivalent with $D_{(v-\eta,v+\eta)}$ but in which all holes are now connected to EXT. The effect of this process on Γ_v is shown in Figure 16 (b). More specifically, all holes represented by D, E and F are "identified" with EXT. As a consequence, the depth of tree representation of Γ_v has been reduced by 2. We then recursively apply this process. In the example, only one more hole is present (represented by H). We again select a simple path from its parent G to H, drill a tunnel in $D_{(v-\eta,v+\eta)}$ that connects the hole to EXT. The result of this process is shown in Figure 16 (c). In particular, the depth of the tree representing Γ_v has been reduced by 1 and all leave nodes are now children of the root node. This implies that Γ_v has been reduced to a disjoint set of disks A, B, C and D. In general, more steps may be needed, each step decreasing the depth of the tree, until the tree has depth 1. Such trees naturally depict disjoint unions of disks, as required, and hence $D_{(v-\eta,v+\eta)}$ is shown to be $\mathcal{I}_3$-equivalent to a number of cylinders.

Step B. Detachment around critical values. We next describe the transformation process around critical values. Consider a critical value v_1 and corresponding set $D_{(v_1-\varepsilon,v_1+\varepsilon)}$. From the case analysis given in [30], it follows that we can identify a working beam $I = [\ell_x, u_x] \times [\ell_y, u_y] \times [v_1 - \varepsilon, v_1 + \varepsilon]$ such that (i) outside I, the sets Γ_v are the same for all $v \in [v_1 - \varepsilon, v_1 + \varepsilon]$; and (ii) inside I, the change from $\Gamma_{v_1+\varepsilon}$ to $\Gamma_{v_1-\varepsilon}$ is described by eight possible cases, as depicted in Figure 17 (each of the four figures can be interpreted from top to bottom, or from bottom to top).

From top to bottom, Cases (a) and (b) in Figure 17 correspond to the removal of a hole and filled region, respectively. From bottom to top, these correspond to the creation of a hole and filled region, respectively. Clearly, we can isotopically transform these case such that $\Gamma_{v_1+\varepsilon} = \Gamma_{v_1-\varepsilon}$. Indeed, for Case (a), we can push out the hole and for Case (b), we can push down the filled region.

This implies that $D_{(v_1-\varepsilon,v_1+\varepsilon)}$ is isotopic to $\Gamma_v \times [0, 1]$ and since this part is isolated, Lemma 4.1 applies. As argued earlier, any Γ_v is $\mathcal{I}_2$-equivalent to a single disk. Hence, in Cases (a) and (b), $D_{(v_1-\varepsilon,v_1+\varepsilon)}$ is $\mathcal{I}_3$-equivalent to an isolated cylinder in $\mathbf{R}^3$, that is, a ball in $\mathbf{R}^3$.

For Cases (c) and (d), we follow a similar approach. From top to bottom, Cases (c) and (d) in Figure 17 correspond to the spliting into two parts of an empty region and full region, respectively. From bottom to top, these correspond to the merging of two empty and full regions, respectively. It should be clear that by applying a $3d$-tube paste transformation in Case (c) and a $3d$-tube cut transformation in Case (d), we can make $\Gamma_{v_1+\varepsilon} = \Gamma_{v_1-\varepsilon}$ and hence obtain that $D_{(v_1-\varepsilon,v_1+\varepsilon)}$ is $\mathcal{I}_3$-equivalent to $\Gamma_v \times [0, 1]$, which in turn is $\mathcal{I}_3$-equivalent to a ball in $\mathbf{R}^3$, as desired.

By performing these transformations between any two critical values and around every critical value, we thus have shown that D can be transformed into a number of balls in $\mathbf{R}^3$, and this in an $\mathcal{I}_3$-preserving way.

After Step C, D is transformed into a single ball in $\mathbf{R}^3$. We further observe that when wires are present in A, an additional $3d$-tube paste transformation results in the elimination of this ball. If no wires are present, however, the ball cannot be eliminated as it is the only $3d$-regular part. We denote by A_3 the result of applying the three-dimensional cleaning process on A_2.

5.2.4 Step 4. Connecting and unknotting wires.

At this point, A_3 is either a single ball, if no wires are present, or A_3 consists of a number of normalised wires connecting $3d$-singular points, possibly together with normalized wires that form knotted wires (when they are not adjacent to $3d$-singular points). We observe the following:

- Different knotted wires of the same profile can be joined together by means of wire cut&paste transformations. We can thus assume that A_3 is $\mathcal{I}_3$-equivalent to a set in which no two distinct knotted wires of the same profile occur.
- If the profile of a knotted wire also occurs as the profile of a wire between $3d$-singular points, one can again use the wire cut&paste transformation to merge these wires. We can thus assume that A_3 is $\mathcal{I}_3$-equivalent to a set in which knotted wires have profiles that do not occur as the profile a wire between $3d$-singular points.
- The possible complex way that wires (either as a knot or between $3d$-singular points) are embedded in $\mathbf{R}^3$ can be simplified by means of the unknotting transformation. In this way, we may assume that A_3 is $\mathcal{I}_3$-equivalent to a set in which every knotted wire has a simple circle in $\mathbf{R}^3$ as it backbone, and every wire between $3d$-singular points has a simple curve as backbone. In addition, none of these backbones are entangled in each other.

Let A_4 be a regular semi-algebraic set in $\mathbf{R}^3$ that is $\mathcal{I}_3$-equivalent to A_3, and in which all wires have been processed as just explained.

5.2.5 Step 5. Bringing in canonical form.

It should be clear that A_4 is already very close to being in canonical form. In fact, when A_4 consists solely of a single ball, we only need to apply an isotopy to transform A_4 into the unit ball $B^3((0,0,0),1)$. If A_4 contains singular points, we can again apply an isotopy that ensures that all these points lie exactly as in the book embedding A_G of the the graph G derived from $\Pi_3(A)$. We note, however, that these singular points may be connected in a different way than in A_G. This can be remedied by applying a sequence of wire cut&paste transformations and unknotting transformations, followed by isotopies. In addition, the remaining knotted wires in A_4 can be isotopically deformed into $A_{\mathcal{P}}$, for the set of profiles $\mathcal{P}$ derived from $\Pi_3(A)$. As a consequence, A_4 is indeed $\mathcal{I}_3$-equivalent to $A_G \cup A_{\mathcal{P}}$, the canonical form of $\Pi_3(A)$.

6 Discussion and concluding remarks

In this paper, we have limited the discussion to *bounded* regular semi-algebraic sets in $\mathbf{R}^3$. This restriction is not essential, however. For unbounded sets, we can obtain a similar characterisation of topological elementary equivalence. Indeed, one can define the cone of the point at infinity in a similar way as for sets in $\mathbf{R}^2$ (see [12], for more details). The point structure $\Pi_3(A)$ can then be extended to $\Pi_3^\infty(A)$, which now includes the cone encoding of the point at infinity. Two unbounded regular sets A and B in $\mathbf{R}^3$ are now $\mathcal{I}_3$-equivalent if and only if $\Pi_3^\infty(A) = \Pi_3^\infty(B)$.

For regular open sets, we get a characterisation of topological elementary equivalence by remarking that A and B are $\mathcal{I}_3$-equivalent if and only if their complements are $\mathcal{I}_3$-equivalent. Indeed, since the complements of regular open sets are regular closed, Theorem 3.6 also gives a characterisation for the regular open case.

The restriction to regular closed (or open) sets is not easily lifted, however. Although we believe that the characterisation of topological elementary equivalence in terms of point structures, as given by Theorem 3.6, carries over to general closed semi-algebraic sets in $\mathbf{R}^3$, additional transformations and a revised notion of the canonical form are required to deal with the one and two-dimensional parts in such sets. In particular, it is unclear how to eliminate obstructions, caused by membranes that separate distinct parts of the semi-algebraic set, when transforming sets into a canonical form.

We further observe that Theorem 3.6 implies that $\mathcal{I}_3$-equivalence (and thus also $\mathcal{H}_3$-equivalence) is a decidable property of regular semi-algebraic sets in $\mathbf{R}^3$. Indeed, in a similar way as for $\mathcal{I}_2$-equivalence [12], the characterisation given in Theorem 3.6 can be easily converted into an effective procedure for testing whether two sets are topological elementary equivalent. Furthermore, the characterisation opens the way to the design of

a multi-tiered cone-based topological query language that precisely captures the expressive power of first-order logic with regard to first-order topological properties of sets in $\mathbf{R}^3$. A similar cone-based languages is known for sets in $\mathbf{R}^2$ [9].

References

[1] M. Aiello, I. Pratt-Hartmann, and J. van Benthem (eds.), Handbook of Spatial Logics (Springer, 2007).
[2] A. N. Whitehead, Process and Reality (The MacMillan Company, New York, 1929).
[3] A. Tarski, What is elementary geometry?, in: The Axiomatic Method, edited by L. Henkin, P. Suppes, and A. Tarski, Studies in Logic and the Foundations of Mathematics Vol. 27 (Elsevier, 1959), pp. 16 – 29.
[4] G. M. Kuper, L. Libkin, and J. Paredaens (eds.), Constraint Databases (Springer, 2000).
[5] J. Bochnak, M. Coste, and M. F. Roy, Real Algebraic Geometry, Ergebnisse der Mathematik und ihrer Grenzgebiete, Vol. 36 (Springer-Verlag, 1998).
[6] A. Tarski, A Decision Method for Elementary Algebra and Geometry (University of California Press, 1951).
[7] E. Grädel, P. G. Kolaitis, L. Libkin, M. Marx, J. Spencer, M. Y. Vardi, Y. Venema, and S. Weinstein, Finite Model Theory and Its Applications, Texts in Theoretical Computer Science. An EATCS Series (Springer, 2007).
[8] L. van den Dries, Tame Topology and O-minimal Structures, London Mathematical Society Lecture Note Series (Cambridge University Press, 1998).
[9] M. Benedikt, B. Kuijpers, C. Löding, J. V. den Bussche, and T. Wilke, A characterization of first-order topological properties of planar spatial data, J. ACM **53**(2), 273–305 (2006).
[10] M. Grohe and L. Segoufin, On first-order topological queries, ACM Trans. Comput. Logic **3**(3), 336–358 (2002).
[11] B. Kuijpers and J. V. den Bussche, On capturing first-order topological properties of planar spatial databases, in: Proceedings of the 7th International Conference on Database Theory (ICDT), , Lecture Notes in Computer Science, Vol. 1540 (Springer, 1999), pp. 187–198.
[12] B. Kuijpers, J. Paredaens, and J. Van den Bussche, Topological elementary equivalence of closed semi-algebraic sets in the real plane, The Journal of Symbolic Logic **65**(4), 1530–1555 (2000).
[13] B. Kuijpers and V. Vianu, Topological queries, in: Constraint Databases, (Springer, 2000), pp. 231–273.
[14] C. H. Papadimitriou, D. Suciu, and V. Vianu, Topological queries in spatial databases, J. Comput. Syst. Sci. **58**(1), 29–53 (1999).
[15] L. Segoufin and V. Vianu, Querying spatial databases via topological invariants, J. Comput. Syst. Sci. **61**(2), 270–301 (2000).
[16] B. Kuijpers, Topological Properties of Spatial Databases in the Polynomial Constraint Model, PhD thesis, University of Antwerp, 1998.
[17] J. Flum and M. Ziegler, Topological Model Theory, Lecture Notes in Mathematics, Vol. 769 (Springer-Verlag, Berlin, 1980).
[18] C. Henson, J. C.G. Jockusch, L. Rubel, and G. Takeuti, First Order Topology, Dissertationes Mathematicae, Vol. CXLIII (Instytut Matematyczny Polskiej Akademi Nauk, 1977).
[19] A. Pillay, First order topological structures and theories, The Journal of Symbolic Logic **52(3)**, 763–778 (1987).
[20] M. Benedikt, G. Dong, L. Libkin, and L. Wong, Relational expressive power of constraint query languages, J. ACM **45**(1), 1–34 (1998).
[21] S. Grumbach and J. Su, Finitely representable databases, J. Comput. Syst. Sci. **55**(2), 273–298 (1997).
[22] S. Grumbach and J. Su, Queries with arithmetical constraints, Theor. Comput. Sci. **173**(1), 151–181 (1997).
[23] E. E. Moise, Geometric Topology in Dimensions 2 and 3, Graduate Texts in Mathematics, Vol. 47 (Springer, 1977).
[24] M. Goresky and R. MacPherson, Stratified Morse Theory, Ergebnisse der Mathematik und ihrer Grenzgebiete, Vol. 14 (Springer, 1988).
[25] F. Geerts, Expressing the box cone radius in the relational calculus with real polynomial constraints, Discrete & Computational Geometry **30**(4), 607–622 (2003).
[26] F. Geerts, B. Kuijpers, and J. V. den Bussche, Linearization and completeness results for terminating transitive closure queries on spatial databases, SIAM J. Comput. **35**(6), 1386–1439 (2006).
[27] C. C. Adams, The Knot Book (W.H. Freeman, 1994).
[28] R. H. Cromwell and R. H. Fox, Introduction to Knot Theory, Graduate Texts in Mathematics, Vol. 57 (Springer-Verlag, Berlin, 1977).
[29] D. Archdeacon, Topological graph theory: A survey, Congressus Numerantium **18**(115), 5–57 (1996).
[30] Y. Shinagawa, T. L. Kunii, and Y. L. Kergosien, Surface coding based on morse theory, IEEE Comput. Graph. Appl. **11**(5), 66–78 (1991).
[31] J. Milnor, Morse theory, Annals of mathematics studies (Princeton university press, 1969).